Organic & Biomolecular Chemistry

Direct Radical Functionalization Methods to Access Substituted Adamantanes and Diamondoids

Journal:	*Organic & Biomolecular Chemistry*
Manuscript ID	OB-REV-09-2021-001916
Article Type:	Review Article
Date Submitted by the Author:	12-Aug-2021
Complete List of Authors:	Weigel, William; University of Iowa, Chemistry; University of California Riverside Dang, Hoang; University of Iowa, Chemistry Feceu, Abigail; University of California Riverside Martin, David; The University of Iowa, Chemistry

Direct Radical Functionalization Methods to Access Substituted Adamantanes and Diamondoids

William K. Weigel, Hoang T. Dang, Abigail Feceu and David B. C. Martin

Contents

Abstract

Adamantane derivatives have diverse applications in the fields of medicinal chemistry, catalyst development and nanomaterials, owing to their unique structural, biological and stimulus-responsive properties, among others. The synthesis of substituted adamantanes and substituted higher diamondoids is frequently achieved via carbocation or radical intermediates that have unique stability and reactivity when compared to simple hydrocarbon derivatives. In this review, we discuss the wide range of radical-based functionalization reactions that directly convert diamondoid C–H bonds to C–C bonds, providing a variety of products incorporating diverse functional groups (alkenes, alkynes, arenes, carbonyl groups, etc.). Recent advances in the area of selective C–H functionalization are highlighted with an emphasis on the H-atom abstracting species and their ability to activate the particularly strong C–H bonds that are characteristic of these caged hydrocarbons, providing insights that can be applied to the C–H functionalization of other substrate classes.

1 - Introduction

1.1 - *Background*

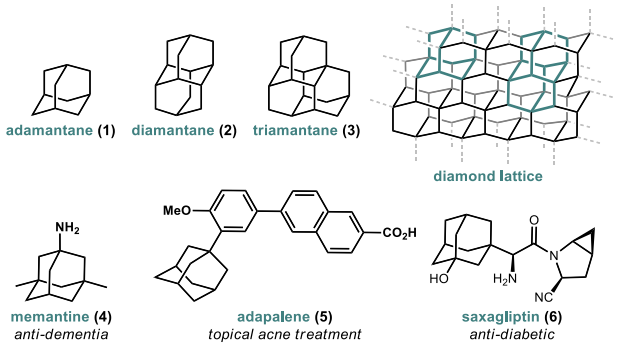

Figure 1. Structure of three simple diamondoids, the diamond lattice and three clinically approved pharmaceutical agents containing adamantane (or small molecule drugs)

Adamantanes are a fascinating class of polycyclic hydrocarbons that have unique physical and chemical properties.[1] As members of the larger family of diamondoids, these caged hydrocarbons are so named because they are nanoscale substructures of the sp^3-hybridized diamond lattice and are characterized by a high degree of symmetry (**Figure 1**).[2,3] Adamantane (**1**, $C_{10}H_{16}$), the simplest member of the diamondoids, has T_d symmetry and thus has only two distinct C–H positions: four equivalent tertiary bridgehead positions connected by six methylene bridges giving rise to its tricyclic cage-like form. Just as diamond is a rigid and mechanically strong allotrope of carbon, diamondoids are rigid and thermodynamically stable molecules of the general formula $C_{4n+6}H_{4n+12}$, ranging from the structurally defined molecules diamantane (**2**), triamantane (**3**), pentamantane etc. to the more loosely defined "nanodiamonds," which have even been detected in interstellar space.[4] Diamondoids from all size regimes continue to be studied for their unique physical and spectroscopic properties and applications in both medicinal and materials applications.[5–7]

Of particular significance is the parent member adamantane (**1**) which, due to its non-planar three-dimensional shape and hydrophobic nature, appears in a number of clinically approved drugs (e.g., memantine **4**), sometimes as a compact lipophilic substituent used to improve binding properties (e.g., adapalene **5**, saxagliptin **6**).[8–13] Adamantane is also frequently used as a bulky alkyl substituent on ligand frameworks[14] such as the first stable crystalline *N*-heterocyclic carbene IAd (**13, Figure 2**) reported by Arduengo,[15] Jacobsen's chiral chromium catalyst for hetero-Diels–Alder reactions (**14**),[16] a Z-selective Grubbs olefin metathesis

Figure 2. Milestones in the Synthesis, Functionalization, and Utilization of Adamantane

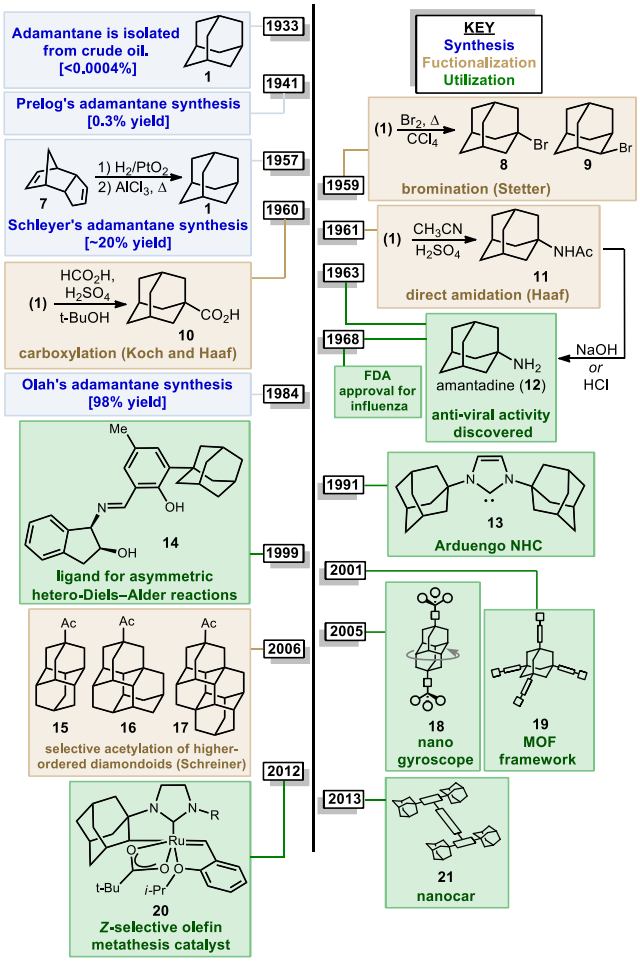

catalyst (**20**),[17] and Davies' PTAD ligand for Rh(II) dimers.[18] Furthermore, the rigid, saturated (and therefore non-conducting) framework of adamantane is commonly used as a scaffold for connecting unsaturated linkers and chromophores in optical materials and nanoscale frameworks (e.g., **18**, **21**).[19–26] These myriad important applications were enabled by several synthetic milestones in the synthesis and substitution of adamantane which make it the readily available starting material it is today.

1.2 - *History*

The caged structure of adamantane was hypothesized in 1924 by H. Decker in a report discussing the structure of diamond, and he dubbed this molecule "decaterpene."[27] Adamantane was then discovered in 1933 by isolation from petroleum sources, although its isolation was extremely limited due to its low natural abundance (~0.0004% petroleum content).[28] Significant interest in the structure of these unusual hydrocarbons in the 1930s led to the first reported synthesis of adamantane by Prelog and Seiwerth in 1941.[29,30] Using classical enolate alkylation reactions for ring closure, Wolff–Kishner reductions and a final double decarboxylation process, they achieved a 1.5% yield of adamantane over the final steps from the previously synthesized Meerwein's ester **22**, **Scheme 1**.[31] Improvements to this route reported by Stetter increased the yield to 6.5%, however the overall strategy still suffered from the multiple steps necessary to remove the functional groups used to assemble the cage.[32,33]

Scheme 1. Synthetic Routes to Adamantane and its Functionalized Derivatives

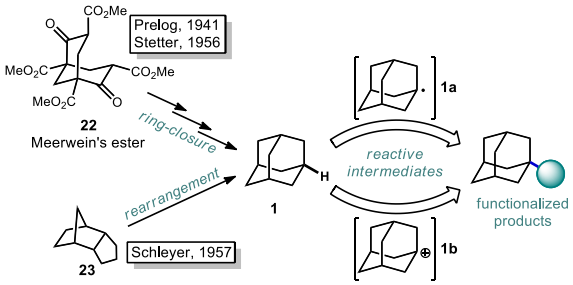

An alternative route to making adamantane was discovered by Paul von Ragué Schleyer in 1957 using a Lewis acid-promoted rearrangement of tetrahydrodicyclopentadiene (**23**). Believed to bear resemblance to the geosynthetic origin of adamantane in petroleum, this groundbreaking isomerization approach was able to improve the yield to 20-40% (**Figure 2**).[32,34] The mechanism of this transformation is proposed to involve a complex series of cationic 1,2 bond migrations and hydride shifts, terminated by the addition of a hydride nucleophile.[35,36] This process is thought to be thermodynamically controlled and proceeds due to the high stability of adamantane (and the 1-adamantyl carbocation **1b**) relative to precursor **23** (and all isomeric carbocations leading to **1b**).[37,38] Related methods have been applied by Schleyer to the synthesis of diamantane (**2**), which is also known as congressane after its appearance as the Congress Emblem of the 1963 London IUPAC meeting.[39,40] Further improvements using superacid catalysis by Olah and coworkers allow the conversion of less stable polycyclic hydrocarbon isomers to diamondoids, providing the most practical method to access diamantane, triamantane and higher diamondoids.[41–43] These methods have been commercialized, facilitating the use of diamondoids in new applications and exploration of their conversion to substituted derivatives.[44,45]

Interest in adamantanes surged again in the 1960s when the first evidence of antiviral activity was reported for a simple amine derivative. In 1961, Haaf *et al.* reported an amidation/hydrolysis sequence to form 1-aminoadamantane,[46,47] also known as amantadine (**12**, **Figure 2**), which was found to display potent anti-influenza A properties in 1964.[48,49] Rimantadine, a chiral aminoalkylated adamantane with anti-viral activity, was similarly introduced in the 1990s. Ultimately, the use of aminoadamantanes to treat influenza was discontinued due to the development of widespread resistance mechanisms. Shortly after amantadine was discovered, the two-carbon homolog memantine (**4**) was synthesized and patented by Eli Lilly and Company as an anti-diabetic.[50] Memantine would later be repurposed as an anti-dementia drug for the treatment of Alzheimer's disease, with FDA approval in 2003, and is still used for this application.[51] Examples of substituted adamantanes in other disease areas include adapalene (**5**),[52] an anti-acne medication, and saxagliptin (**6**), a DPP-4 inhibitor used in the treatment of diabetes.

With the exception of 1-aminoadamantanes, which can be directly synthesized via a Ritter or nitration reaction, the synthesis of substituted adamantanes typically relies on halogenated intermediates that can be converted to the corresponding radical **1a** or carbocation **1b** for substitution (**Scheme 1**). The tertiary carbocation **1b** is unusually stable due to hyperconjugation with filled bonding orbitals within the rigid cage while radical **1a** is destabilized due to its inability to relax to a more stable pyramidal conformation. For the bromination of adamantane, the ratio of 1-bromoadamantane (**8**) and 2-bromoadamantane (**9**) depends on the reagents employed, with a phase-transfer catalyst system reported by Schreiner and Fokin providing nearly complete selectivity for the more substituted product.[53,54] Similarly, different conditions allow diamantane to be converted to a mixture of medial 3º-bromide (**24**), apical 3º-bromide (**25**) and 2º-bromide products (**26**, **Scheme 2**). Substitution of these alkyl halides can be accomplished via S_N1-type substitution with a variety of carbon and heteroatom nucleophiles and by conversion to the corresponding radical by traditional methods. These methods, which are reliable and provide access to discrete substitution patterns by isolation of the appropriate halide intermediate, nonetheless require multistep sequences and the separation of byproducts at each step to provide the desired diamondoid products.

Scheme 2. Effect of Reaction Conditions on Apical and Medial Selectivity in Diamantane Bromination

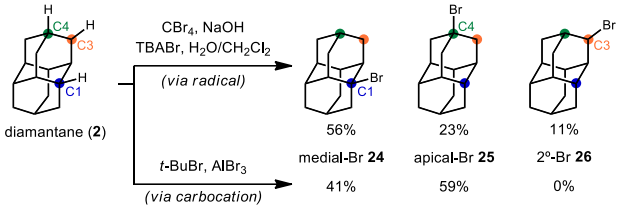

Alternatively, the direct substitution of adamantane has long been a test-bed for direct C–H functionalization methods, particularly because of the unusually high bond dissociation energies (BDEs) of this class of molecules (96 and 99 kcal/mol for 2º and 3º C–H bonds, respectively).[55] As a result, H-atom abstractors with high reactivity are required, including *O*-centered radicals derived from peroxides and photoexcited diaryl ketone species.[56,57] A central challenge that emerges is the issue of selectivity between non-equivalent 2º and 3º positions of adamantane, higher order diamondoids (e.g., **2**, **3**; **Figure 1**) and substituted derivatives (e.g., drug molecules **5**, **6**). This challenge has placed limitations on the complexity of reaction partners, where multiple different types of C–H bonds would lead to complex mixtures of substitution products. Solutions to this challenge have involved the careful study of mechanistic details and identification of key features such as polar effects and polarizability that enable the selective apical arylation and acetylation of higher diamondoids as reported by Albini and Schreiner (see **15-17**, **Figure 2**), both discussed in greater detail below. Based on these mechanistic insights, the direct conversion of diamondoid C–H bonds to C–C substituted products can be carried out in a selective manner, and often provides the most efficient access to these versatile building blocks. Over 60 years after Schleyer's synthesis, the range of applications of adamantanes and higher order diamondoids appears only limited by a chemist's creativity and their ability to produce substituted derivatives in a controlled, selective and efficient manner.

1.3 - *Scope of the Review*

Traditional methods for the conversion of diamondoid C–H bonds to C–halide, C–O, C–N and other C–X bonds are numerous and have been reviewed elsewhere.[58–66] Likewise, reactions for the use of halo- and hydroxyadamantanes as intermediates for substitution have been the focus of previous literature summaries. This Review will focus on direct methods for the conversion of diamondoid C–H to C–C bonds proceeding via radical intermediates. These transformations, spanning over 50 years of published work, are organized according to the reaction classes and this review will highlight the diverse species used for the key H-atom abstraction step. While many papers describe a single example of adamantane as a substrate, particular attention will be given to reports that focus on the functionalization of diamondoids as a class of substrates.

2 - Acylations

Acyladamantanes, molecules featuring a direct C–C bond between adamantane and the carbonyl group of a ketone, ester or aldehyde, are one of the earliest derivatives to be made by a direct C–H to C–C radical functionalization. Acyladamantanes are useful intermediates that can be further modified (e.g., by reductive amination) and while many traditional methods have been applied for their synthesis, most rely on a pre-functionalized adamantyl substrate and/or harsh conditions for accomplishing the necessary introduction of the acyl group. Therefore, direct methods for forging C–C bonds to adamantanes that eliminate the need for pre-functionalization are desirable. By accessing the reactive nucleophilic adamantyl radical, direct acylations of adamantane are achievable and fall into three main categories described in this section: chlorocarbonylation, acetylation and formylation.

2.1 - *Chlorocarbonylation*

One of the first examples of radical-mediated C–H to C–C functionalization was described by Tabushi and coworkers in 1968 (**Scheme 3**).[67] This seminal report involved the radical chlorocarbonylation of adamantane using oxalyl chloride and a benzoyl peroxide radical initiator, leading to acylated intermediate **27** as illustrated below. The adamantyl radical **1a** is generated using chlorine radical which is initially produced via homolysis of peroxide **29** and then propagated according to the mechanism shown (**30**→**31**→Cl•). Following methanolysis of **27**, a mixture of methyl 1- and 2-adamantanecarboxylates (**28**, 49% yield, 55:45 rr) was obtained. The yield reported by the authors was 82% BRSM (based on the recovered starting material, in this case, adamantane). After statistical correction, this distribution of regioisomers corresponds to a reactivity ratio of 3.67:1 favoring the tertiary adamantyl positions. This preferential reactivity of the tertiary C–H bonds of adamantanes was also observed in prior radical halogenations by Smith and Williams, a critical process that helped showcase the potential utility of radical-based methods early on.[68] One factor that leads to the preferential reactivity of the 3° position is reduced steric hindrance, where approach to the 2°-C–H groups leads to significant 1,3-diaxial interactions that are absent at the 3° position.

Investigating this system further, Tabushi later showed that using adamantanes with different substituents at the 1-position altered the ratio of 3°:2° chlorocarbonylation products on a steric basis (OMe > CO_2Me > Me > CN > H).[69] This product ratio ranged from 1.2:1 for unsubstituted adamantane (R=H) to 5.7:1 (R=OMe). Interestingly, these substituent effects were drastically different from those observed in prior radical halogenations by Owens et al. using trichloromethyl radical.[70] While Tabushi saw correlation only to steric size, Owens found that the same substituents influenced the regioselectivity through both steric and polar effects according to a linear free-energy relationship expressed by the Taft equation.

2.2 - *Acetylation*

In a related investigation by Tabushi and coworkers, they demonstrated in 1973 that adamantane can be selectively acetylated using an excess of diacetyl under irradiation to give 1-acetyladamantane (**32**) as the sole regioisomer (**Scheme 4**).[71,72] The C–H abstracting species is believed to be the triplet-excited state of diacetyl since no acetylation

Scheme 3. Benzoyl Peroxide Intitated Chlorocarbonylation Using Oxalyl Chloride

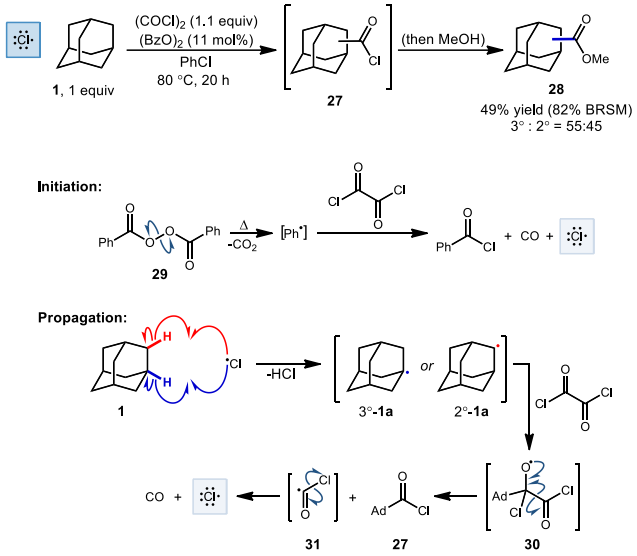

occurred in the presence of pyrene, a known quencher of diacetyl phosphorescence via energy transfer.[73] Despite also being a quencher, the presence of oxygen actually increased the rate of acetylation and the production of the 2-acetyladamantane (**33**) and 1-adamantanol, the autooxidation product. The increase in photoacetylation rate and loss of selectivity is attributed to the generation of reactive methyl radicals which form in a decarboxylative process after oxygen and diacetyl react (**Eq 1**).

Tabushi also showed that the photoacetylation of diamantane proceeded selectively at the methine positions using diacetyl under conditions similar to those used for adamantane.[74] However, while adamantane features four equivalent methine positions, higher ordered diamondoids possess two or more nonequivalent 3º positions. In the case of diamantane featuring two apical and six medial positions (see positions

Scheme 4. Photoacetylation of Adamantane Using Diacetyl

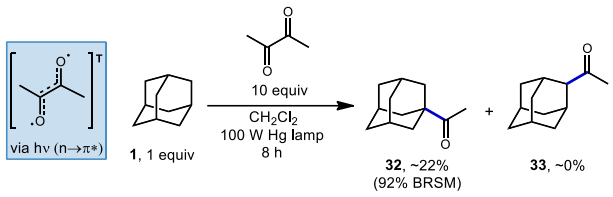

Oxidative Diacetyl Decompostion

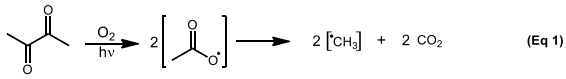

Diacetyl Quenching Studies (2 h)

Conditions	1-acetyl adamantane (%)	2-acetyl adamantane (%)	1-adamantanol (%)
N_2	13.8	--	--
N_2, pyrene	0	--	--
O_2	28.6	12.3	8.3

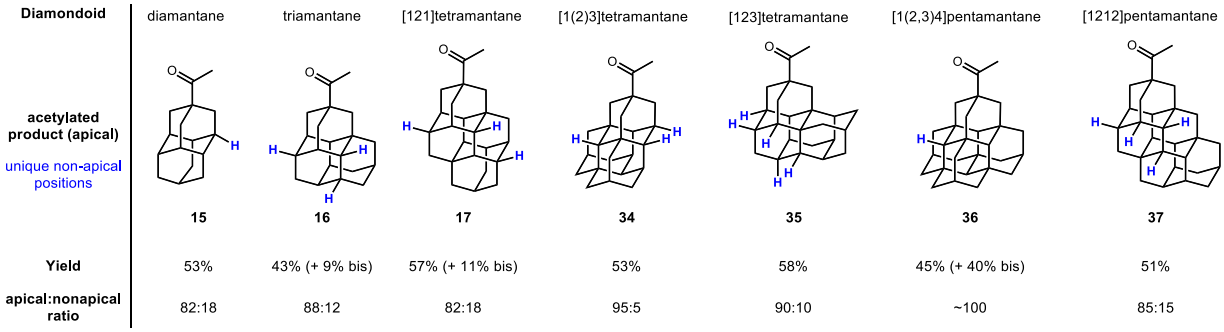

Figure 3. Apical photoacetylation products in higher-ordered diamondoids. Other unique non-apical tertiary C–H postions are indicated in blue.

labeled C1 and C4 in **Scheme 2**), photoacetylation using diacetyl favored mono-acetylation at the apical position over the medial position in a 5.5:1 ratio. Acetylation of the methylene positions and bis-addition products were not observed.

Schreiner and coworkers later showed that apical selectivity during photoacetylation under similar conditions is maintained in even higher ordered tri-, tetra-, and pentamantanes despite an increase in the number of possible medial positions (see **Figure 3**).[75] For instance, despite the unique number of 3°-C–H positions increasing from two in diamantane **15** to four in triamantane **16** and [121]tetramantane **17**, acetylation of the apical position is still favored over the other medial positions in an ~5:1 ratio. Even higher apical selectivity is observed in the acetylation products for [1(2)3]tetramantane **34** and [123]tetramantane **35** (despite **35** having six unique C–H positions).[76] [1(2,3)4]pentamantane (**36**) showed near complete apical selectivity and resulted in a significant amount of bis acetylated product as well. The selectivity in these reactions is largely governed by the relative steric accessibility of the apical positions over the more hindered medial positions.

2.3 - *Formylation*

Scheme 5. Light-Enabled Formylation of Adamantane Using Sulfonyl Aldoxime

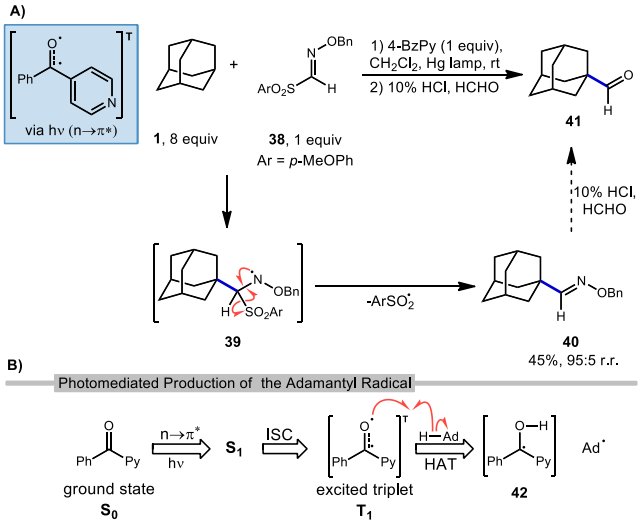

Recently, Kamijo et al. have reported a method for formylating unactivated C(sp^3)–H bonds in many substrates including adamantane through the intermediacy of an *O*-benzylaldoxime **40** (**Scheme 5a**).[77] Although the formylated product is not produced directly in a single step, the overall transformation introduces a carbonyl group, similar to other reactions in this section. In this reaction, 4-benzoylpyridine (4-BzPy) is used with a mercury lamp to generate a photoexcited triplet (4-BzPy^T) which acts as the C–H abstractor for adamantane (**Scheme 5b**). The triplet is produced through light-dependent n to π* transition between the singlet ground (S_0) and excited state (S_1) followed by intersystem crossing (ISC) to the excited triplet (T_1), a common manifold for other ketone and quinone catalysts. While the resulting radical species **42** could in principle turn over in a photocatalytic process by transferring a hydrogen atom or a proton/electron stepwise to regenerate the ketone 4-BzPy, they are typically used in a stoichiometric amount and likely form a 1,2-diol dimer byproduct.

After HAT with 4-BzPy^T, Kamijo revealed that the resulting adamantyl radical can readily intercept aldoxime **38** to give amino radical **39**. Fragmentation of this intermediate results in loss of arylsulfonyl radical to form the *O*-benzylaldoxime product **40** in 45% isolated yield high regioselectivity for the methine position (95:5). This aldoxime can then be converted to the formylated product **41** using a solution of formaldehyde in aqueous HCl. While this final hydrolysis step was not performed on adamantyl product **40**, it is expected to proceed smoothly based on data for other substrates in this work.

2.4 - *Esterification and Amidation*

In 2018, Doyle and coworkers used nickel and photoredox catalysis to enable direct C–C bond formation between unactivated alkanes and chloroformate **43** to form ester products.[78] Adamantanecarboxylate ester **44** was synthesized in 46% yield with a slight preference for the less substituted regioisomer (2°:3°=1.3:1) using the conditions shown in **Scheme 6**. The chloroformate is thought to undergo an oxidative addition with $L_nNi(0)$ **45** to form $L_nNi(II)(Cl)(CO_2R)$ **46** followed by SET with the excited iridium photocatalyst to produce a Ni(III) species **47**. Photolytic cleavage liberates a chlorine radical which performs HAT with adamantane to generate the adamantyl radical (**48**→**49**). Addition of the adamantyl radical forms nickel complex **50** which undergoes reductive elimination to give the ester product and the resulting Ni(I) species **51** is turned over by single electron reduction from Ir(II) species **52**.

As seen earlier in this section with respect to chlorocarbonylation, this reaction also demonstrates the tendency of chlorine radical to perform HAT with low regioselectivity. The slight preference for the formation of the ester product at the bridge position may occur due to reversible radical capture by nickel and a bias for reductive elimination of the secondary alkyl fragment. This is thought to occur in other nickel-catalyzed reactions involving the capture of 2° and 3° adamantyl radicals (see **Scheme 45**).

Scheme 6. Esterification of Adamantane with Chloroformate 43 Using Dual Ni/Ir Photoredox Catalysis

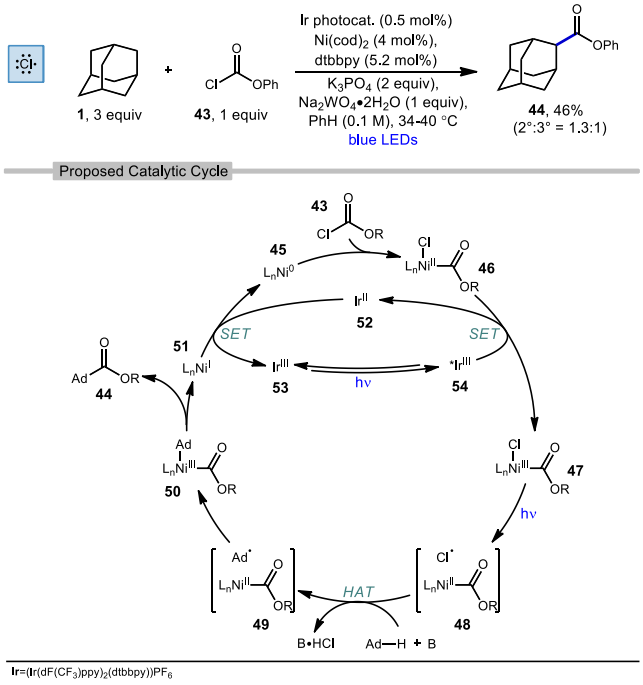

Li and coworkers have recently reported an amidation of adamantane and other alkanes using aromatic isocyanides and di-*tert*-butylperoxide (DTBP) (**Scheme 7**).[79] Three isocyanides with differing aryl substituents were used with adamantane to afford amides **56**-**58** in low to moderate yields (33–53%). The reaction is thought to first involve the ferrocene-catalyzed formation of *tert*-butoxyl radical **59** which produces the adamantyl radical via HAT. Addition of the adamantyl radical into the isocyanide forms iminyl radical intermediate **60** that is then trapped by oxygen as hydroperoxide **61**. Finally, homolytic O–O bond scission to oxygen-centered radical **62** is followed by hydrogen abstraction and tautomerization to give the final amide product. The products were isolated as single regioisomers, however one would also expect the formation of the isomeric 3º product based on the typical selectivity of the *tert*-butoxyl radical in related reactions (e.g., 2:1, **Scheme 46**).

Scheme 7. Iron-catalyzed Radical Amidation of Adamantane via Aryl Isocyanides

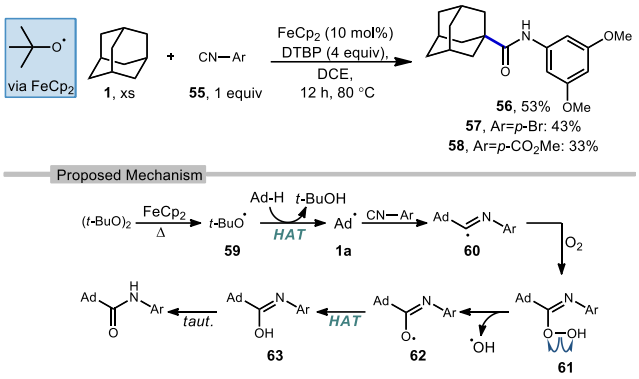

3 - Carbonylation with Carbon Monoxide

Scheme 8. General Scheme for Carbonylations of the Adamantyl Radical Using Carbon Monoxide

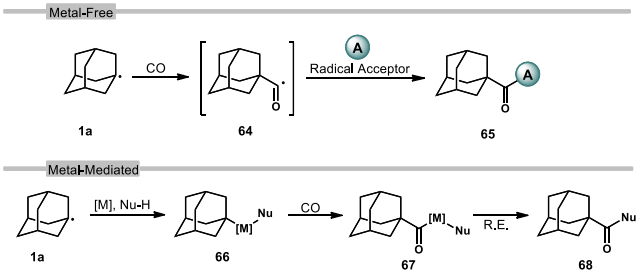

Carbonylation reactions of adamantane using carbon monoxide (CO) are employed to access acyladamantane products, similar to the acylative transformations described in the previous section. However, the processes described below primarily involve the direct, metal-free reaction of adamantyl radical **1a** with CO in solution to give the adamantyl acyl radical **64** (**Scheme 8**, top). Various strategies for arriving at this acyl radical have been developed and then combined with different radical acceptors to obtain carbonylated products **65**. The adamantyl radical can also be coupled to CO through transition metal-catalyzed processes such as insertion (**66**→**67**; **Scheme 8**, bottom) and reductive elimination (**67**→**68**) to provide carboxylate derivatives. These carbonylative transformations are presented together in this section.

3.1 - *Carboxylation using NHPI*

The C–H functionalization of saturated hydrocarbons using carbon monoxide, although attractive, is quite challenging due to a general lack of selectivity and low conversion of starting material.[80–82] Work done by Ishii in 1998 showed that oxidation of polycyclic alkanes in the presence of air and carbon monoxide can produce carboxylated products using a catalytic free radical mechanism (**Scheme 9**).[83] *N*-Hydroxyphthalimide (NHPI, **69**) is used as a catalyst in the presence of O_2 to generate the (phthalimide-*N*-oxyl (PINO, **70**) radical without photoactivation and under mild conditions. However, selectivity is quite poor when using adamantane as the hydrocarbon and a mixture of carbonylated and oxygenated products **71-76** were obtained.

Scheme 9. Oxidative Carbonylation of Adamantane Using the Phthalimide-*N*-oxyl Radical

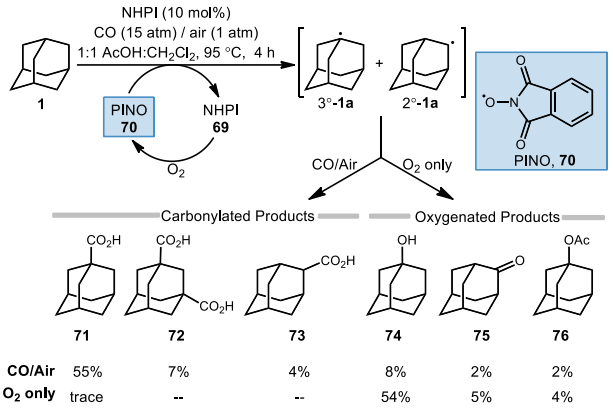

A likely mechanism begins with generating the reactive intermediate PINO from NHPI in the presence of O_2. The PINO radical will abstract a hydrogen at either the secondary or tertiary position of adamantane to give the 3°-**1a** and 2°-**1a** adamantyl radicals. These radicals are intercepted with CO forming the acyl radical **64** and upon subsequent reaction with O_2, eventually generates carboxylic acids **71-73**. Interestingly, when 1-adamantanecarbocylic acid (**71**) is used as the starting material, the dicarboxylate **72** was formed in 57% yield. Alternatively, the adamantyl radicals can instead react directly with O_2 to give the oxygenated products 1-adamantanol (**74**), 2-adamantanone (**75**), and 1-acetoxyadamantane (**76**). When only O_2 is used, these oxygenated products are favored. Overall, the reaction selectivity is not significantly impacted by other changes in conditions (e.g., solvent and temperature).

3.2 - *Photocatalytic Carbonylation*

In 2011, Ryu and Albini reported a three-component coupling reaction between adamantane, carbon monoxide, and Michael acceptors using photocatalytic methods (**Scheme 10**).[84] This multi-component process generated unsymmetrical ketones with tetrabutylammonium decatungstate (TBADT, **78**) as the photocatalyst and a xenon lamp as the UV light source. A l:1.3 mixture of the 1- and 2-adamantane ketosuccinates (**79**) was obtained, although the yield was relatively low (35%) compared to other cyclic hydrocarbon substrates.

Scheme 10. Three-component Synthesis of Adamantyl Ketones Using Decatungstate Photocatalysis

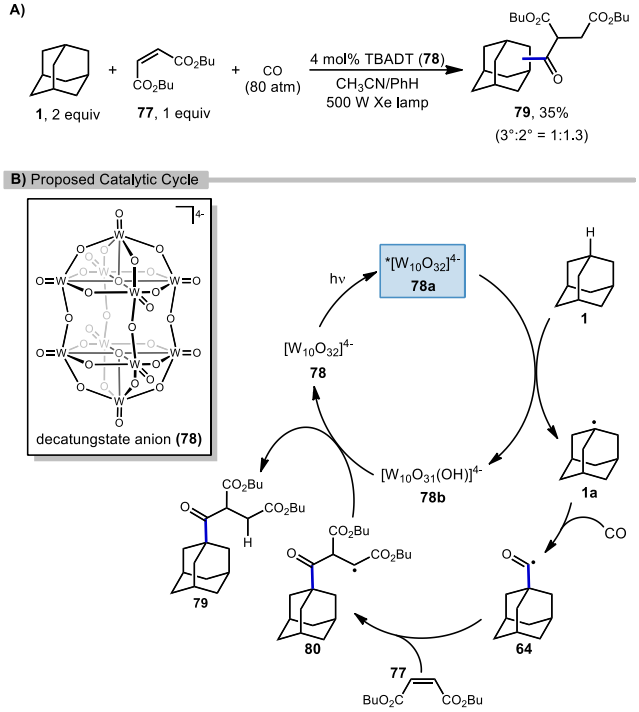

The proposed catalytic cycle for the C–H functionalization of adamantane using a tandem carbonylation-addition process is illustrated in **Scheme 10**. Upon irradiation of TBADT, the excited photocatalyst **78a** abstracts a hydrogen from adamantane generating adamantyl radical **1a**. Carbonylation results in the acyl radical **64** followed by a Giese addition to give succinyl radical **80**. Reduction of intermediate **80** by the reduced photocatalyst **78b** turns over the catalyst and produces the desired functionalized adamantane product **79**, either via HAT or an electron-transfer/proton-transfer mechanism.

3.3 - *Transition Metal-Catalyzed Carbonylation*

The use of transition metals for C–H activation methods that include carbonylation is an attractive route for generating products containing carbonyl groups. However, commonly used second- and third-row transition metal catalysts (e.g., Ru, Rh) are expensive and require complex organometallic preparations, limiting their use.[85–87] First row transition metals like nickel and copper are excellent alternatives due to their low toxicity, low cost and relative abundance.[88]

With this in mind, Wu et al. reported the first copper-catalyzed carbonylative C–H activation in 2016 using a variety of alkanes and amides to generate imides.[89] Wu employed a Cu(I) species and DTBP to selectively functionalize adamantane at the tertiary position with *N*-methylacetamide (**81**), likely via the *tert*-butoxyl radical, generating the imide **82** in 31% yield (**Scheme 11**, top). The acylation of adamantane required a cosolvent and proceeded in lower yield than other hydrocarbons.

Scheme 11. Metal-catalyzed Adamantane Amidations Using Carbon Monoxide

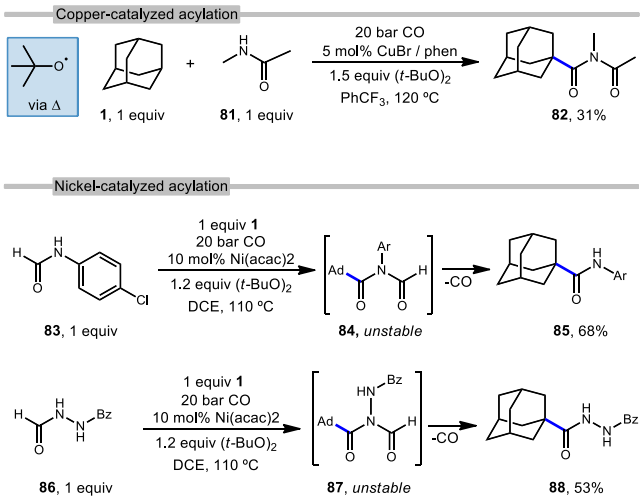

In addition to copper, nickel catalysis has also previously been reported for the activation of inert C(sp^3)–H bonds.[90] Recently, Yufeng Li et al. developed a Ni-catalyzed carbonylation of unreactive alkanes such as adamantane with formamides to obtain amide products.[91] **Scheme 11** (bottom) illustrates two selective carbonylations employing adamantane. The first reaction uses an equimolar amount of formanilide **83** to give the amide product **85** in modest 68% yield while the second utilizes *N*-formylbenzohydrazide (**86**) which gave the corresponding diacylhydrazine **88** in 53% yield. Similar to the work done by Wu and coworkers with copper, DTBP is homolytically cleaved with the help of nickel to form the key reactive intermediate, the *tert*-butoxyl radical. However, unlike Wu's work, the Ni-catalyzed insertion of CO generates imide intermediates (**84, 87**) which are unstable and quickly undergo loss of the formyl group as CO to give the observed amide or hydrazide product.

Scheme 12. Esterification of Adamantane Using Palladium-Catalyzed Oxidative Carbonylation

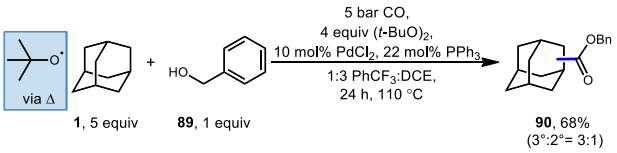

Carbon monoxide can also be used for the synthesis of adamantyl esters. Lei and coworkers reported a palladium-catalyzed oxidative carbonylation method for hydrocarbons including adamantane using benzyl alcohol (**89**) and carbon monoxide to generate one carbon-homologated esters (**Scheme 12**).[92] The reaction proceeds at relatively low CO pressure (5 bar) to give ester product **90** in good yield (68%) with preference for activation at the bridgehead position of adamantane (3°:2° = 3:1). Once the adamantyl radical is generated by HAT, it is proposed to intercept a Pd-CO complex to form an acyl palladium species (potentially in equilibrium with acyl radical) that reacts with benzyl alcohol to afford the product.

3.4 - *Metal-Free Oxidative Radical Carbonylation*

Scheme 13. Metal-Free Esterification of Adamantane Using DTBP

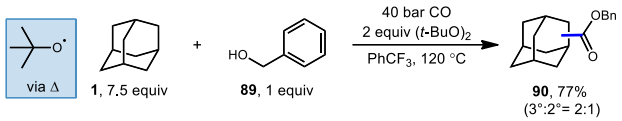

Lei et al. have also developed a metal-free oxidative carbonylation of alkanes via direct C–H bond activation using DTBP in the presence of carbon monoxide and benzyl alcohol to generate esters (**Scheme 13**).[93] A variety of alkanes including adamantane underwent efficient conversion to corresponding benzyl ester products like **90**. While the reaction proceeded in good yield, the regioselectivity of the H-atom abstraction step was rather low, giving a 2:1 ratio of 3°:2° product in 77% yield. Like many examples in this Review, the key HAT step here is facilitated by the *tert*-butoxyl radical, and the nucleophilic adamantyl radical is proposed to react directly with CO. This approach offers a convenient metal-free alternative to palladium-catalyzed method discussed in the previous section; however, it requires a significantly higher pressure of CO to intercept the radical intermediate.

4 - Alkylation via Alkene Addition Reactions

Scheme 14. General Giese Reaction Involving Adamantane

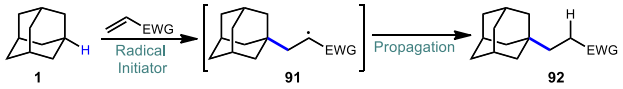

The addition of the adamantyl radical to an alkene acceptor is a convenient method of effecting adamantane alkylation. In this category, Giese-type reactions, which involve trapping of a carbon centered radical with an electrophilic alkene (**Scheme 14**), are frequently used. The resonance-stabilized radical intermediate, commonly an α-acyl radical, can undergo reduction and protonation (**91**→**92**) or further reactions such as chain propagation or tandem addition steps which lead to a diverse array of transformations.

Adamantane alkylation has traditionally been accomplished using pre-functionalized halo-adamantanes together with organometallic methods such as Wurtz and Grignard reactions or via Lewis acids such as $FeCl_3$ and $AlCl_3$.[58,94,95] However, avoiding the need for preactivated starting materials through direct C–H activation of adamantane is an attractive option both in terms of atom economy and step count. As such, there are many examples of Giese-type additions to alkenes that proceed by a radical C–H abstraction to directly generate the necessary adamantyl radical.

4.1 - *First Peroxide-Catalyzed Alkene Additions*

In 1974, the earliest report of a direct C–H alkylation of adamantanes was published by Tabushi and Fukunishi, wherein they described the reaction of 1,3-dimethyladamantane (**93**) with ethylene gas using 5 mol% DTBP for initiation (**Scheme 15**).[96] With 2 bar ethylene, 1-alkylated 3,5-dimethyladamantane products **94-97** were formed in 22.5% yield (with the remainder being unreacted adamantane) with nearly exclusive regioselectivity for the bridgehead position. Among the products, the ethyl product **94** was predominantly formed (89%) although smaller quantities of the telomeric butyl and hexyl products (**95** and **96**) were also generated. These telomeric products suggest a radical chain mechanism is likely where the radical adds to the alkene and the resulting 1º alkyl radical abstracts from the next molecule of adamantane or (at a slower rate) adds to another alkene. While higher pressures of ethylene only led to slightly higher conversion to products, they resulted in a noticeably higher distribution of oligomer products. Adamantane (**1**) also underwent alkylation to form the ethyl and butyl products (~11% yield) but

increasing the ethylene pressure beyond 5 bar led to near quantitative recovery of starting material. Other alkenes such as 1-hexene, 1-octene, cyclohexene and cyclooctene were also reacted with 1,3-dimethyladamantane to give moderate yields of 1:1 alkylation adducts (up to 26% yield). This is the only example of an alkylation reaction with simple unactivated alkenes as radical acceptors.

Scheme 15. Alkylation of Dimethyladamantane via Radical Addition to Ethylene

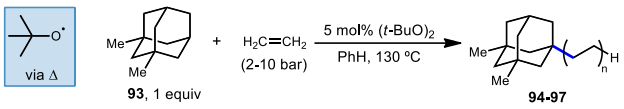

	Ethylene Pressure (bar) 2	5	10
3,5-dimethyladamantane conversion (%)	22.5	29.6	25.3
Products	**Distribution (%)**		
94, 1-ethyl-3,5-dimethyladamantane (n=1)	89.0	69.7	33.5
95,1-butyl-3,5-dimethyladamantane (n=2)	10.5	17.0	23.9
96,1-hexyl-3,5-dimethyladamantane (n=3)	0.5	1.8	4.8
97,1-octyl-3,5-dimethyladamantane (n=4)	0	0.4	1.1

Tabushi and Fukinishi would later go on to report that peroxide catalysis could also be used with different electron-withdrawn olefins to give alkylated adamantane products **99-103** (**Scheme 16**) in moderate to good yields.[97] The reactive species responsible for the production of the adamantyl radical in these reactions is once again *tert*-butoxyl radical and is generated at elevated temperatures using DTBP.

Scheme 16. Early DTBP-Catalyzed Giese Reactions with Electron Deficent Olefins

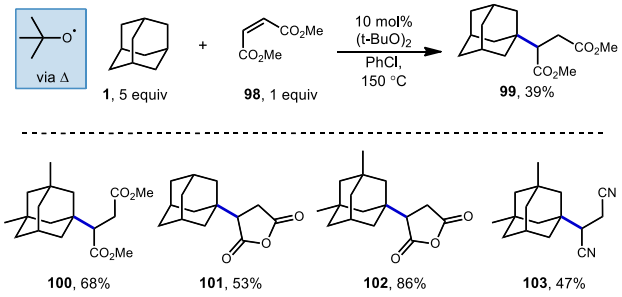

4.2 - *Photochemical Alkylation*

There are several examples of photochemical adamantane alkylation reactions that occur under mild conditions and tolerate a variety of electron-deficient alkene reaction partners. These reactions are enabled by the inclusion of a photosensitive additive, the properties of which change significantly between ground state and excited state, facilitating electron transfer or H-atom transfer. Compounds such as benzophenone necessitate the use of high energy UV light, however, other photocatalysts and dual catalyst systems have been developed that function under visible light.

In 2000, Albini and coworkers developed a photochemical radical alkylation to access α-thiosulfones from ketene dithioacetal *S*,*S*-dioxides (**Scheme 17**, top).[98] α-Thiosulfones are convenient synthetic intermediates that can be used for several key transformations, such as desulfurization[99] and pyrolysis to obtain carbonyl derivatives.[100] With stoichiometric amounts of benzophenone, one equivalent of (*E*)-1-(methylthio)-1-[(4-methylphenyl)-sulfonyl)]propene (**104**), excess adamantane and UV light, the thiosulfone product **105** was obtained in 90% yield as a single diastereomer determined by NOE spectroscopy. The stereoselectivity was dependent on the steric bulk of the alkyl radical; cyclohexane was alkylated in 89% yield but with lower diastereoselectivity (d.r.=82:18). Alkylation was selective for the tertiary bridgehead position and trace amounts of phenyladamantane, bis-adamantane, 1-adamantanol, and 2-adamantanone were also observed. These oxygenated trace products were the result of reaction with residual oxygen.

Scheme 17. Diastereoselective Alkene Additions Using Benzophenone

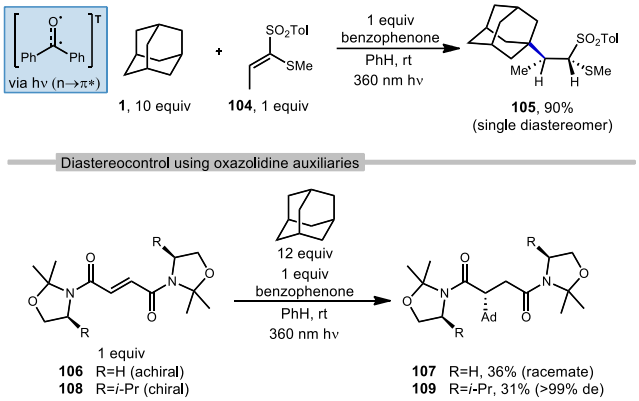

Albini et al. used similar conditions to study radical additions to fumaric acid diamides adorned with oxazolidine chiral auxiliaries to generate functionalized products with a high degree of diastereoselectivity.[101] As shown in **Scheme 17** (bottom), chiral and achiral oxazolidines were tested with excess adamantane and benzophenone as photosensitizer. Irradiation at 360 nm resulted in the triplet excited state of benzophenone which provides the 3° adamantyl radical and addition to achiral fumaryloxazolidine (R=H, **106**) gave the amidated adamantane product (**107**, 36% yield) as a racemate. The use of a substituted chiral oxazolidine (R=*i*-Pr, **108**) provided the reaction with a good degree of stereocontrol and the amide product **109** was obtained as a single diastereomer (31% yield, >99 de).

Scheme 18. Photochemically Mediated Radical Additions of Adamantane to α,β-Unsaturated Nitriles

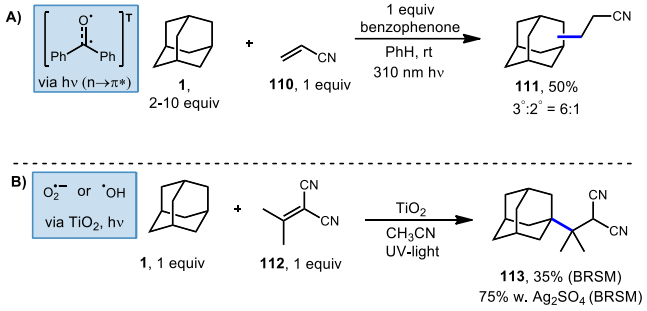

A common and particularly reactive class of electron-deficient olefins are the α,β-unsaturated nitriles. These substrates commonly participate in Giese additions to produce adducts possessing nitrile moieties that map onto natural products and other metabolites of interest.[102] However, accessing alkyl nitriles directly through traditional methods has limitations due to toxicity of the organometallics and cyanide salts required.[103,104] Albini's photochemical benzophenone platform provides a much safer route to the alkylation of these alkenyl nitriles.[105] Using this approach, cyanoethyl adamantanes were synthesized using excess adamantane, one equivalent of acrylonitrile (**110**) and one equivalent of photosensitizer (**Scheme 18**, top). The resulting products were formed as a mixture of the two adamantyl regioisomers (**111**, 50% yield) in a 6:1 ratio. The yield was determined by gas chromatography and the reported isolated yield was somewhat lower.

Albini also tested TiO_2, a known heterogeneous photo-oxidant in the presence of oxygen or water.[106] As shown in **Scheme 18** (bottom), isopropylidene malononitrile and adamantane were treated with TiO_2 and irradiated under UV light. A yield of 35% of product **113** was obtained based on recovered starting material. Oxygenated products were also observed which were attributed to reaction with oxygen. A higher yield of 75% was obtained when silver sulfate was included as an oxidant.

Scheme 19. Light-Driven Radical Additions to Cyclic Enones

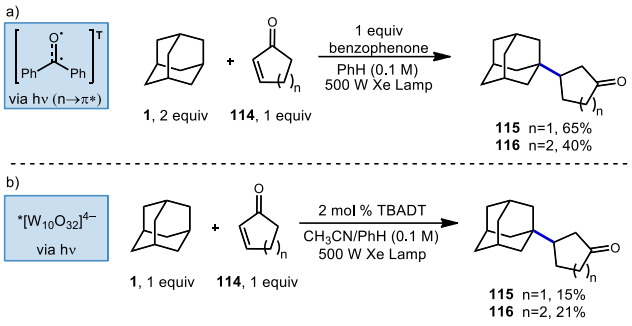

Albini and coworkers continued to study new methods for photochemical C–H functionalization of hydrocarbons and in 2006, they reported two additional methods to synthesize β-alkylated ketones using UV activation (**Scheme 19**).[107] The adamantyl radical was generated via HAT using either stochiometric benzophenone or catalytic TBADT. When using benzophenone as the abstractor, only 1-adamantyl derivatives were observed and cyclic ketone products **115** and **116** were generated with yields of 65% and 40%, respectively. The high performance of adamantane at low concentration is explained by relative rates of radical addition to the enone. In a report for radical addition to a similar electron deficient olefin, the rate of addition by adamantyl radical (k=3.0x10^8 M^{-1}s^{-1}) was found to be approximately two orders of magnitude faster than cyclohexyl radical (k=3.3x10^6 M^{-1}s^{-1}).[108]

Switching the photocatalyst to TBADT resulted in lower yields, with cyclopentanone product **115** giving 15% yield and the cyclohexanone product **116** giving 21% yield. The authors do not comment on the selectivity of the reaction with TBADT; however, based on low the selectivity of TBADT in other similar reactions (**Scheme 10**), both regioisomers would be expected to be present. The proposed reaction mechanism involves a direct H-atom abstraction by the excited photocatalyst as opposed to energy transfer or electron transfer pathways.

In 2019, our research group demonstrated a photochemical alkylation strategy using a broad range of alkenes and a variety of adamantanes with remarkable selectivity (>20:1 r.r.) for the 3º position (**Scheme 20a**).[109] Inspired by previous work done by MacMillan and coworkers involving the functionalization of α-hydroxy C–H bonds, [110] this approach uses a dual catalytic system involving an iridium photocatalyst (Ir(dF(CF$_3$)ppy)$_2$(d(CF$_3$)bpy)PF$_6$ **135** (see **Scheme 22**) in tandem with a quinuclidine-based HAT catalyst. Optimal results were obtained using a novel quinuclidinol-derived HAT co-catalyst **136** with a more electron-withdrawing sulfonate group. When these catalysts are used together under blue light irradiation, adamantane reacts with electron-deficient alkenes such as dehydroalanine derivative **117** to give the alkylated product **118** in 89% yield (**Scheme 20a**)

Alkylation proceeded smoothly for alkenes featuring a number of electron-withdrawing groups such as ketones, esters, nitriles, and sulfones (**119-125**, 65-94% yield). The robustness of the reaction also enabled a wide of adamantanes to perform well in this reaction (typically 60-75% yield). These included adamantanes substituted at the 1-position **126-128** (alkyl, aryl, hydroxyl, halide, nitrile, acetyl), diamantane **129**, 2-adamantanone, and drug derivatives such as *N*-Boc amantadine and *N*-Boc memantine, which all reacted with high regioselectivity.

In this system, an electrophilic quinuclidinium radical cation (**136a**) is produced that is well suited for HAT from hydridic C–H bonds like those found at the methine positions of adamantane. Notably, this favorable polarity matching in the transition state of the HAT step enables the selective functionalization of stronger C–H bonds over weaker ones with impressive regioselectivity. Complex adamantane substrates such as **130** (**Scheme 20b**) featuring multiple weaker C–H bonds were alkylated with phenyl vinyl sulphone **131** to give the 3º adamantyl product **132** in 70% yield and >20:1 r.r. The reaction also showed resilience during direct competition experiments between equimolar amounts of adamantane and many other diverse substrates. These substrates featured a range of C–H bonds (e.g., 2º and 3º alkyl, benzyl, amidyl, formyl, etc.) including large polyfunctional substrates (e.g., limonin and progesterone) and were added without significantly competing with or diminishing yields of adamantane product **121**.

Scheme 20. Site-Selective Alkylation of Adamantane Using Dual Photoredox Catalysis

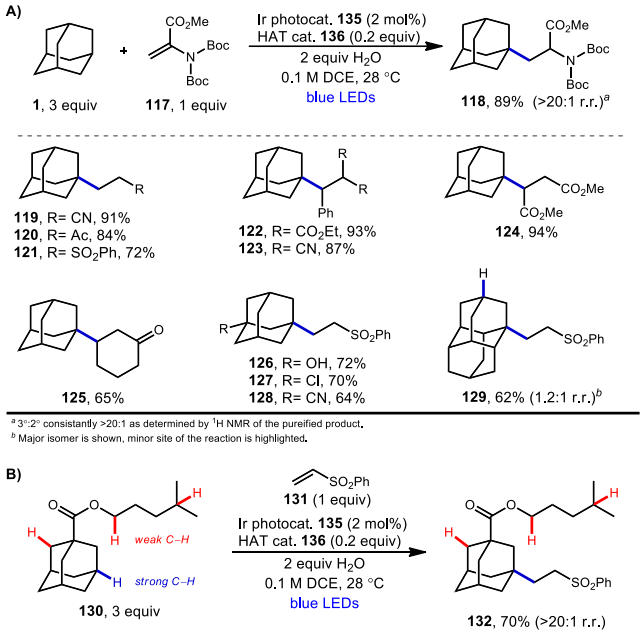

A comparison of this catalyst system with other photocatalytic HAT systems described in this Review was carried out, as shown in **Scheme 21**. The intermolecular competition between adamantane and octanal only favored the reaction of adamantane with the quinuclidine catalyst, whereas all other catalysts were less efficient and led to ketone **134** as the major product. This remarkable selectivity is attributed to the preference for the most electron-rich "hydridic" C–H bond being activated, enhanced by the positive charge on abstractor **136a** and the optimized electron-withdrawing nature of the sulfonate substituent.

Scheme 21. Intermolecular Competion Studies With Different Catalyst Systems

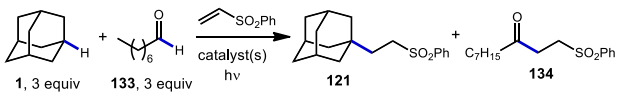

Entry	Catalyst system	Yield **121**	Yield **134**	Selectivity
1	**Ir-1**(**135**), **Q-1**(**136**)	63%	14%	**4.5:1**
2	PT (**187**)	13%	26%	1:2
3	TBADT (**78**)	8%	41%	1:5.1
4	**Ir-2**, NBu_4OBz	7%	34%	1:4.9
5	Acr (**150**), HPO_4^{2-}	7%	7%	1:1

Ir-1=(**Ir**(dF(CF$_3$)ppy)$_2$(d(CF$_3$)bpy)PF$_6$; **Q-1**=quinuclidin-3-yl benzenesulfonate; **PT**=5,7,12,14-pentacenetetrone; **TBADT**=tetrabutylammonium decatungstate; **Ir-2**=(**Ir**(dF(CF$_3$)ppy)$_2$(dtbbpy)PF$_6$; **Acr**=Nicewicz acridinium photocatalyst

The driving force for the process is the formation of the relatively strong N–H bond in quinuclidinium **136b** following the HAT event with adamantane (N–H BDE ~100 kcal/mol or higher).[111] This effect was leveraged by installing an electron withdrawing substituent on quinuclidine to further increase the N–H BDE and increase the efficiency of the reaction in terms of both yield and reaction time.

Scheme 22. Proposed Dual Catalytic Cycle for Adamantane Alkene Additions

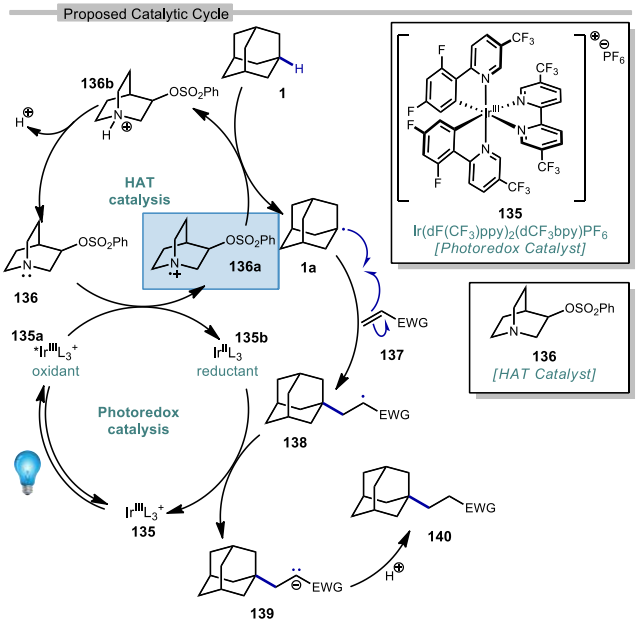

Another iridium photoredox-catalyzed alkylation, which uses chlorine radical to generate the adamantyl radical, was reported a few months prior to the quinuclidine-based method discussed above. While most implementations of iridium(III) photocatalysts use relatively inert counter ions such as hexafluorophosphate, Barriault and coworkers showed that using a catalyst containing a chloride counter ion, [Ir(dF(CF$_3$)ppy)$_2$(dtbbpy)]Cl, chlorine radical can be generated. This catalyst was used to alkylate adamantane using dimethyl maleate (**98, Scheme 23**) to form the adamantyl succinate **99** in 61% yield (3°:2°=62:38).[112] The reaction is thought to proceed similarly to the dual catalytic cycle depicted in **Scheme 22** with chlorine radical serving in place of quinuclidine radical cation **136a** to perform HAT, leading to the diminished regioselectivity. Nonetheless, this strategy was effective for a

Scheme 23. Radical Addition to Dimethylmaleate Using an Iridium Photocatalyst

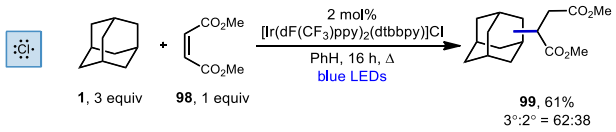

variety of other hydrocarbons, ethers, aldehydes and heteroatom-activated starting materials.

Nicewicz and Alexanian have also recently developed a general strategy for organic photoredox-catalyzed C–H abstraction from an array of aliphatic substrates followed by trapping with a variety of radical acceptors using an acridinium photocatalyst, phosphate salt and blue light (**Scheme 24**).[113] This general process reported in 2018 allowed for the direct diversification of C–H bonds into new C–N, C–S, C–X and C–C bonds. The methodology uses a highly oxidizing acridinium photocatalyst **150** to oxidatively generate oxygen-centered phosphate radicals capable of doing C–H abstraction of aliphatic compounds including adamantane. When using an aryl-adamantyl adapalene precursor with 3-butenone (**141**) as the radical acceptor, ketone product **148** was formed in 45% yield. This reactivity extended beyond Giese type reactions to non-alkene radical acceptors such as 4-(trifluoromethyl)benzenesulfonyl azide (**142**) and *N*-fluorobenzenesulfonimide (NFSI, **143**). *N*-Phthalimidyl memantine underwent fluorination to give fluorinated product **146** in 86% yield while azidation to provide **145** was possible in 55% yield. Unsubstituted adamantane was also converted to the azide in 75% yield.

Scheme 24. Photochemical C–H Functionalizations of Adamantane Using Acridinium Catalyst 150

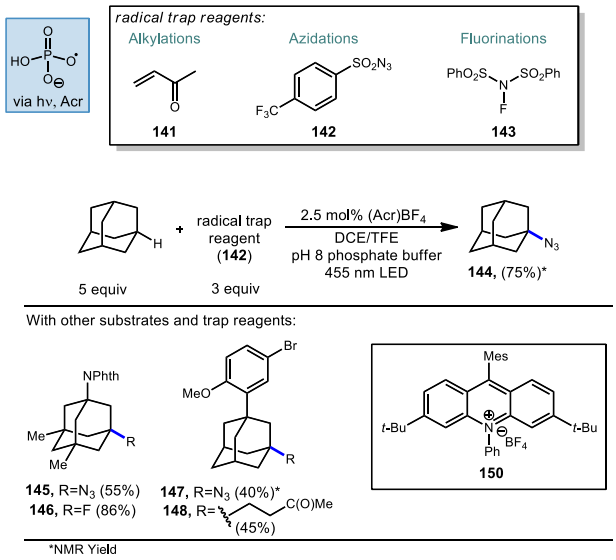

Recently, Knowles, Alexanian and coworkers have also demonstrated a method for functionalizing unactivated C(sp^3)–H bonds using a phosphate and a photocatalyst. Unlike the work from Nicewicz discussed above involving a phosphate radical created through single-electron oxidation, a thorough mechanistic investigation indicates a mechanism that proceeds via multisite-proton-coupled electron transfer (MS-PCET).[114] Using an iridium photocatalyst together with a monobasic phosphate salt, adamantane and its substituted derivatives were alkylated with 1,1-bis(phenylsulfonyl)ethylene (**152**, **Scheme 25**) in moderate to good yield (**153-155**, 58-80%). A protected memantine derivative was also alkylated in 40% yield. NMR titration experiments and crystallographic evidence indicate the formation of a noncovalent 1:1 Ir(III)-phosphate complex via hydrogen bonding between 3,3'-bipyridyl positions and the

phosphate oxygen (see **156**). The reaction is belived to be dependant on the formation of this complex since virtually no alkylation was observed when a competitive binder (fluoride ion) was included or when an Ir(III) catalyst with fluorinated 3,3'-bipyridyl positions was used.

Similar to HAT, PCET generates the adamantyl radical via homolytic C–H bond cleavage. However, unlike HAT, which involves the movement of a proton and an electron together to a single location (one orbital), MS-PCET involves the movement of the proton and electron to two separate orbitals. Quenching studies suggest a mechanism involving the excitation of the pre-associated Ir(III)-phosphate complex followed by a concerted PCET process with the adamantane substrate to give the adamantyl radical, the reduced Ir(II) photocatalyst and the protonated phosphate base (see **157**). Once generated, the adamantyl radical proceeds to react with the olefin and Ir(II) species in a manner similar to the process shown in **Scheme 22**.

Scheme 25. Alkene Addition via Photocatalytically Induced Proton-Coulped Electron Transfer

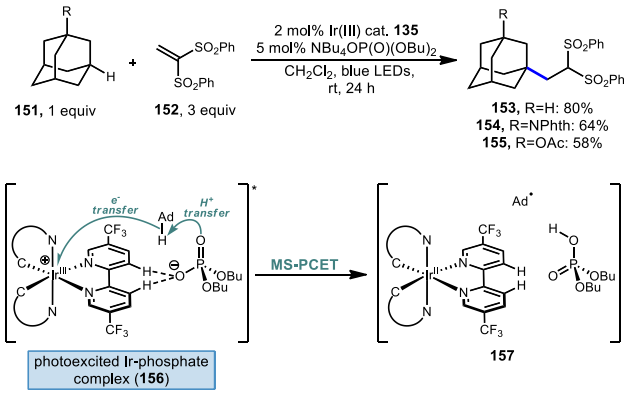

4.3 - *Additional Non-Photochemical Alkylations*

A catalytic oxyalkylation of alkenes with adamantanes and other alkanes was reported by Ishii et al. in 2001 using the PINO radical as the reactive intermediate and a cobalt co-catalyst in the presence of molecular oxygen. [115] This reaction resulted in oxyalkylated products in both the hydroxylated and ketone oxidation state (**Scheme 26a**). Under optimized conditions, methyl fumarate (**158**) and adamantane gave 98% conversion with a 78% yield (71/29 ratio of hydroxy product **159** and ketone product **160**. A variety of alkenes were also tested using dimethyl adamantane with yields ranging from modest to excellent however in most cases, a mixture of products was observed (**Scheme 26b**, **161**-**165**).

A proposed mechanism is summarized in **Scheme 26c**. These reactions are thought to be initiated by single-electron transfer (SET) to $Co(acac)_3$ to give a Co(II) species that undergoes reaction with O_2 to form a Co(III)-O_2 complex. HAT from NHPI to this cobalt complex generates the incipient PINO radical. PINO then goes on to generate the adamantyl radical via another HAT process. Adamantyl radical addition into the alkene **158** affords alkyl radical intermediate **166** which is quickly trapped by O_2 leading to hydroperoxide **167**. This hydroperoxide undergoes decomposition by Co ions giving the alkoxy radical intermediate **168**. Additional HAT from either NHPI or adamantane yields the hydroxylated

Scheme 26. Cobalt-catalyzed Oxyalkation of Alkenes with Adamantane

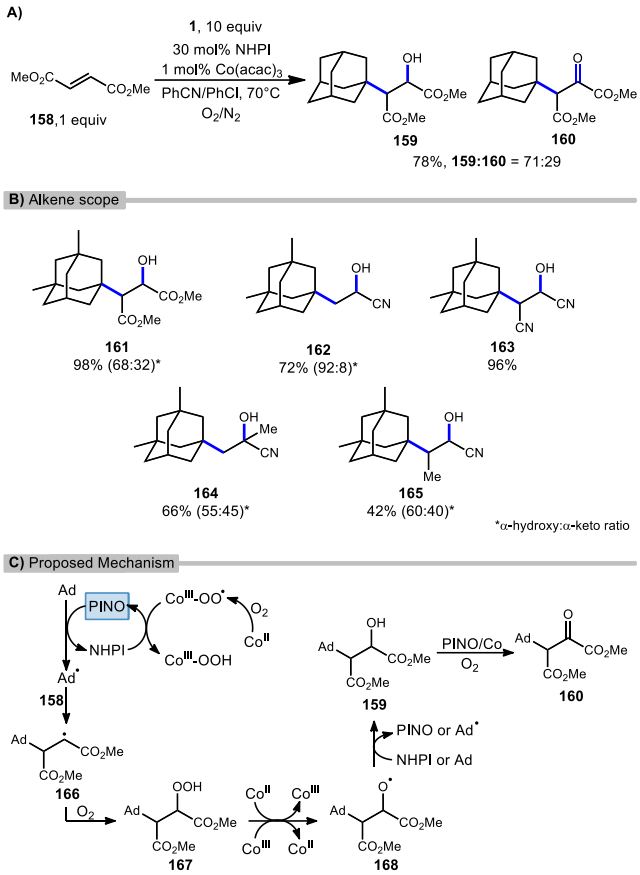

product **159**. Further oxidation to α-keto ester **160** is then possible in the presence of O_2 with the assistance of $Co(acac)_3$ and PINO.

Roberts and coworkers reported a fascinating metal-free radical cascade reaction using allyloxyl intermediate **176** as the key radical chain-propagating reagent (**Scheme 27**).[116] In this work, the reaction of interest involved excess adamantane, *N*-methylmaleimide as the acceptor (**169**, NMM), "acetal reagent A" **170**, and di-*tert*-butyl hyponitrite (TBHN) as a radical initiator. With adamantane, the final ester product **171** was obtained in 50% yield as a 79:21 regiochemical mixture favoring the tertiary position. Product formation proceeds as part of a complex radical cascade enabled by acetal reagent A.

Scheme 27

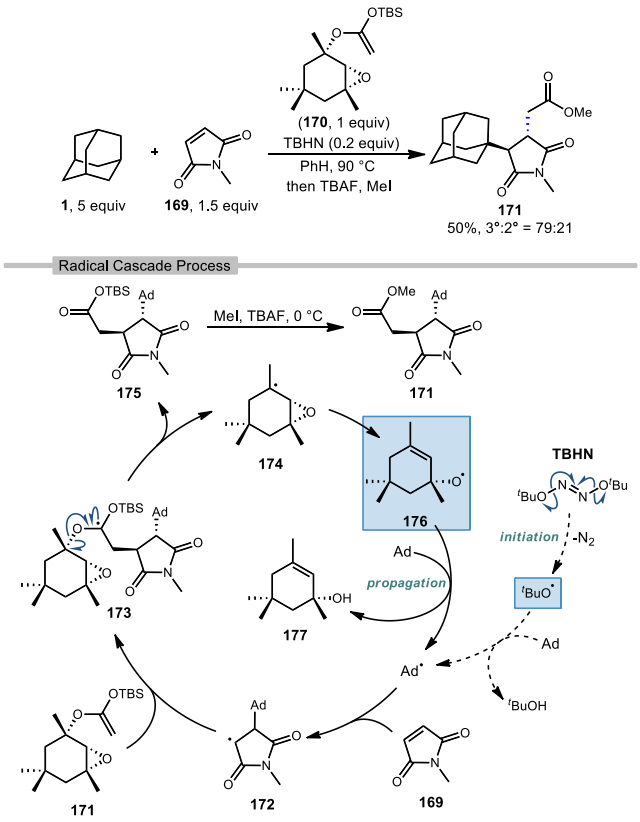

5 - Addition-Fragmentation Processes with Alkene and Alkyne Reagents

Scheme 28. General Addition-Fragmentantion Sequences

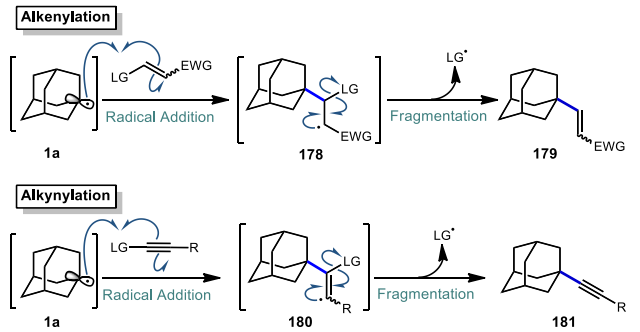

The addition-fragmentation sequence (**Scheme 28**) is well represented in the realm of radical chemistry and has been reported in a variety of cases involving the adamantyl radical.[117] After C–H abstraction, the resulting adamantyl radical **1a** then adds into an appropriate radical acceptor such as an alkene leading to a β-adamantyl radical intermediate **178** which undergoes fragmentation to an alkenylated adamantane product **179**. Alkynes, which are valuable building blocks in organic synthesis and as important structural compounds in both material science and chemical biology,[118,119] also behave similarly but instead involve fragmentation of the analogous vinyl radical (**180**).

The reactions discussed in this section involve addition into electron-deficient alkene or alkyne acceptors to accomplish alkenylative, allylative, or alkynylative transformations. Commonly, radical acceptors feature an electron-withdrawing group to aid in stabilizing radical intermediate **178** (or **180**) as well as a leaving group that promotes a facile fragmentation immediately following addition. These reactions may be accomplished by both metal-free and metal-mediated radical processes. We note that the formylation reaction discussed in Section 2.3 proceeds via a similar fragmentation following addition to a C=N radical acceptor.

5.1 - *Decarboxylative Alkenylation*

Scheme 29. Decarboxylative Alkenylation of Adamantane Using Cinnamic Acid

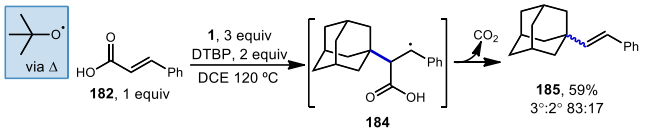

Sun et al. demonstrated that styrenyl adamantanes (**185**, **Scheme 30**) can be made using cinnamic acid (**182**) in the presence of DTBP and heat.[120] In this case, homolytic thermolysis of DTBP results in *tert*-butoxyl radical that acts as the C–H abstractor giving rise to the reactive adamantyl radical. This reaction is then thought to proceed via initial radical addition to form benzylic radical **184**, followed by loss of carbon dioxide and an additional H-atom. This addition-fragmentation process is selective for the tertiary adamantyl position, favoring it over the secondary position and formed the styrenyl product in an 83:17 ratio, consistent with other HAT processes involving the *tert*-butoxyl radical.

5.2 - *Photochemical Allylation*

Scheme 30. 5,7,12,14-Pentacenetetrone Catalyzed Allylation Using 1,2-bis(phenylsulfonyl) Propene D

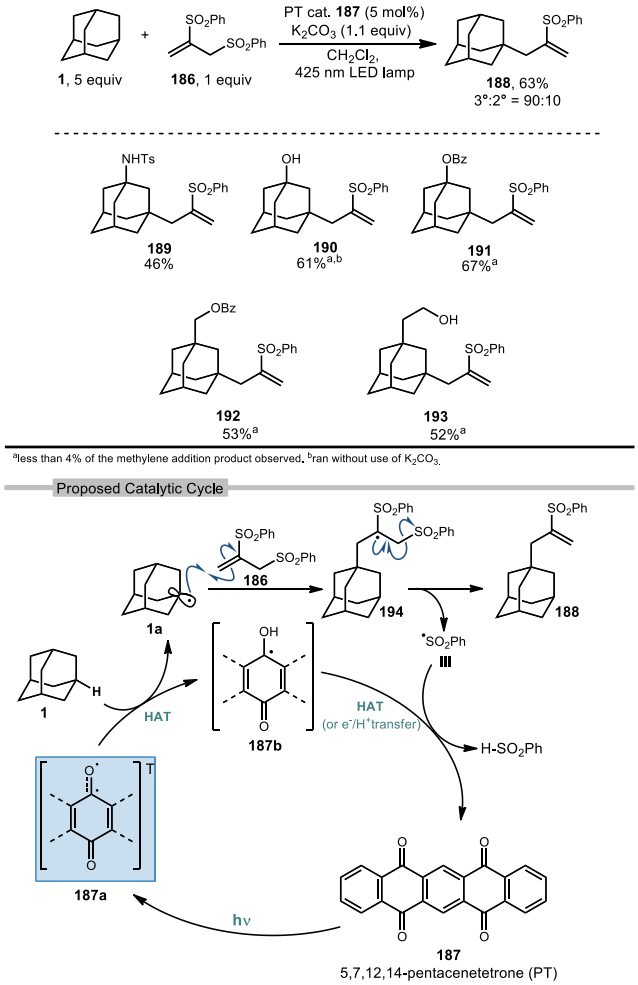

Allylation of adamantanes has been demonstrated using 1,2-bis(phenylsulfonyl) propene (**186**, **Scheme 30**) as an allylating agent.[121] The adamantyl radical is generated using 5,7,12,14-pentacenetetraone (PT, **187**) with visible light irradiation. The excited state **187a**, with biradical character similar to photoexcited benzophenone, is a competent C–H abstractor, presumably leading to semiquinone form **187b**.[122–124] Adamantyl radical **1a** then intercepts the electrophilic sulfonylated propene to generate radical intermediate **194**. Fragmentation and transfer of a H-atom from the PT catalyst results in allylated adamantane, **188** and benzenesulfinic acid as a byproduct. Under these conditions, **188** was isolated in 63% yield with the allylated methine being favored in a 9:1 ratio over the methylene position. These conditions also were tolerated by a range of substituted adamantanes. Using substituted adamantanes **189-193** generally favored C–H functionalization at one of the remaining methine positions at a ratio of >95:5.

Wang and coworkers recently developed a method for the directed allylation of adamantane using a tethered amidyl radical via intramolecular 1,5-HAT (**202**, **Scheme 31**).[125] When the oxyarylamide group is tethered at the 2º position of adamantane **195**, allylation using sulfone **196** occurred at the 3º position (via 3º C–H abstraction) to give allyl adamantane **197** in 73% yield. Moving the tether to the 3º position of adamantane **198** led to allylation at the 2º position (2º C–H abstraction) in 67% yield, indicating that in both cases the highly favored 1,5-HAT was driving the selectivity.

The amidyl radical is generated photocatalytically using green LEDs to excite eosin Y (EY, **200**) which undergoes SET to the prefunctionalized adamantane featuring di-nitroaryloxy amide **195**. The resulting radical anion, **201**, then fragments to give the key amidyl radical **202**. Similar to a Hofmann–Löffler–Freytag reaction, this remote amidyl radical was used to generate the adamantyl radical **203** via a 1,5 C–H abstraction.[126] Interception of the allyl sulfone by the adamantyl radical and subsequent fragmentation of **204** gives the 3° allylated adamantane.

Scheme 31. Directed Photocatalytic Allylation of Adamantane via Tethered Amidyl Radical Intermediates

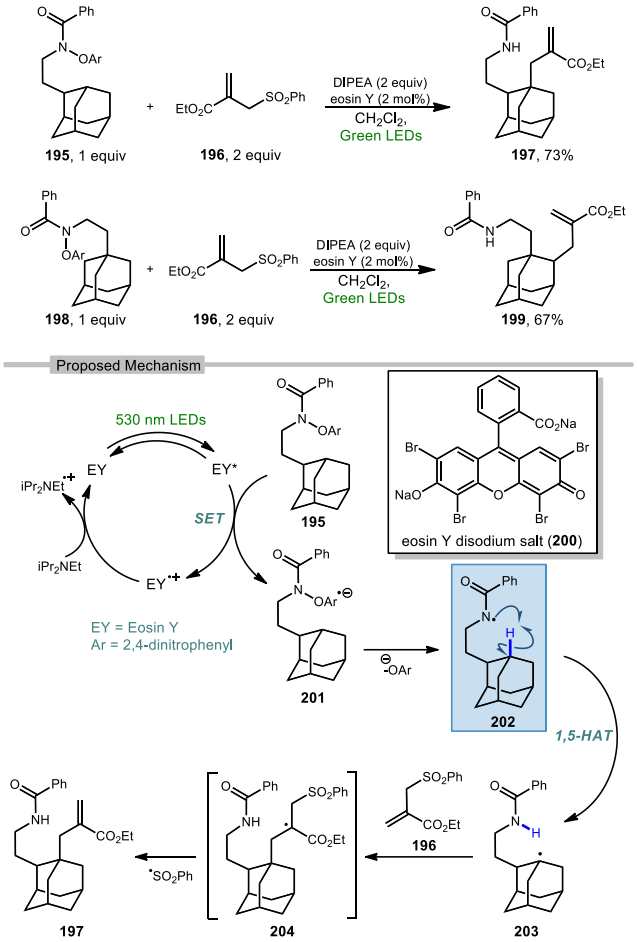

5.3 - *Photochemical Alkenylation*

Addition/fragmentation sequences also work well in the preparation of alkenylated adamantyl derivatives through the formation of a new C(sp^3)–C(sp^2) bond. In 2014, Inoue and Kamijo used benzophenone for the photochemical alkenylation of substituted adamantanes using *trans*-1,2-bis(phenylsulfonyl)ethylene **206** to the give corresponding alkenylated sulfonyl-adamantanes (**207-209**, **Scheme 32**).[127] The formation of these vinyladamantanes proceeded with high selectivity for the methine position with good yields in MeCN under irradiation from a 100W mercury lamp. The presence of proximal heteroatoms (X=O, N) typically activates adjacent C(sp^3)–H bonds through hyperconjugation with the nearby lone pair.[56] C(sp^3)–H bonds of heteroatom-substituted carbons are therefore typically selectively abstracted over other aliphatic positions as seen in the reaction with ambroxide (**210**). Interestingly, oxa- and azaadamantanes (**211** and **212**, respectively) were the only exceptions to this rule according

to Inoue and Kamijo, presumably because no hyperconjugation between the lone pair and C–H bond can occur within the rigid cage-like structure.[128]

Scheme 32. Photochemical Alkenylations of Substituted Adamantanes Using Benzophenone

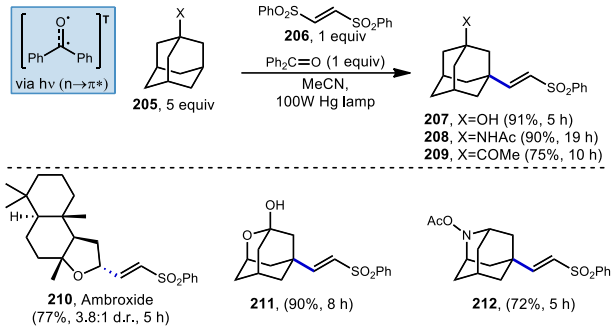

5.4 - *Metal-Catalyzed Alkenylation*

A copper-catalyzed radical addition/cyclization of various unactivated cycloalkanes including adamantane with alkynyl-phosphine oxide **213** to give cyclic alkenylated products was reported by Zhao et al. in 2018 (**Scheme 33**).[129] The cyclic benzo[*b*]phosphole oxide product **214** forms from two sequential C–H abstractions and the formation of two new C–C bonds. The initial *tert*-butoxyl radical is formed after the Cu(I)-assisted homolysis of DTBP with heating. Addition of the adamantyl radical into electron-deficient alkyne **213** results in the key alkenyl radical intermediate **215**. This radical can then follow two regiochemically divergent paths both leading to the same product. In Path A, *ortho*-addition of the alkenyl radical leads to delocalized radical **216**. In Path B, *ipso*-addition of the alkenyl radical results in the 4-membered spirocyclic intermediate **217** which opens to give phosphorus-centered radical **218**, followed by *ortho*-readdition to give aryl radical **216**. By either proposed pathway, radical **216** can re-aromatize via oxidation with Cu(II)(O*t*-Bu) to give the product and regenerate Cu(I).

Scheme 33. Copper-catalyzed Alkenylative Cyclization Using Alkynyl-Phosphine Oxide 213

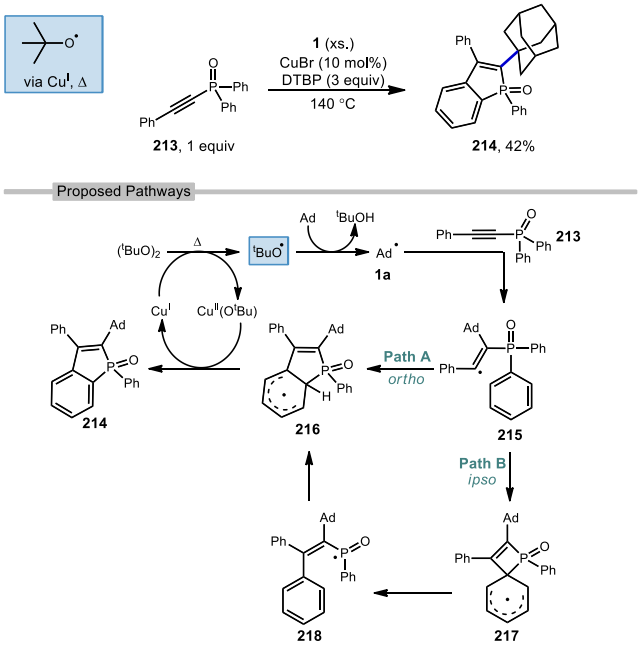

5.5 - *Alkynylation*

An early example of a metal-free C–H alkynylation was reported by Fuchs using alkynyl triflone **219** to functionalize a variety of C–H bonds, including those on adamantane (**Scheme 34**).[130,131] Using AIBN and heat for initiation, the tertiary alkynylated adamantane **220** was obtained in 60% yield. The authors note the possibility of two mechanistic pathways depending on the regiochemistry of the initial adamantyl radical addition to the alkyne. In the case of β-addition (Path A), sulfonyl vinyl radical **221** undergoes homolytic fragmentation to give vinylidene carbene **222** and (trifluoromethyl)sulfonyl radical **223**. Once formed, the vinylidene carbene undergoes a Fritsch−Buttenberg−Wiechell rearrangement to the alkynylated product.[132] Alternatively, α-addition to the alkyne (or a 1,2-shift from **221**) affords β-sulfonyl vinyl radical **224**. This intermediate can then eject (trifluoromethyl)sulfonyl radical to form the substitution product. In both cases the transient sulfonyl radical undergoes further fragmentation to sulfur dioxide and trifluoromethyl radical which propagates the reaction by C–H abstraction, forming fluoroform as the byproduct.

Scheme 34. Adamantane Alkynylation Using Alkynyl-Triflone 219

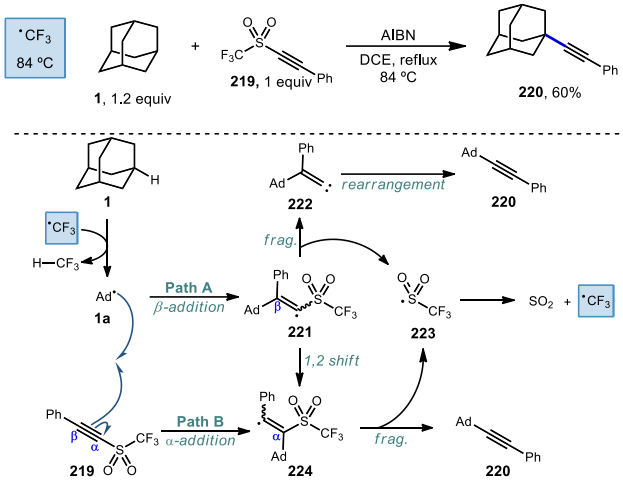

Alkynylative transformations of substituted adamantanes using metal-free photocatalytic methods have also been demonstrated using tosyl-(trimethylsilyl)acetylene **227** with benzophenone and a mercury lamp (**Scheme 35**).[133] Upon irradiation with UV light, the triplet excited state is generated which then abstracts a hydrogen atom from the tertiary position of adamantane, generating the adamantyl radical. This intermediate then reacts with the electron-deficient alkyne and subsequent release of the toluenesulfinyl radical from alkenyl intermediate **231** generates the alkynylated adamantyl product, similar to the Fuchs example above. Under these conditions, 1-adamantanol (**74**) was alkynylated in 86% yield and *N*-Boc-protected amantadine was alkynylated and deprotected to the free amine using TFA in 73% yield over 2 steps (**225**→**228**→**229**).

Scheme 35. Photochemical Alkynylation of Substituted Adamantanes Using Tosyl-(trimethylsilyl)acetylene 226

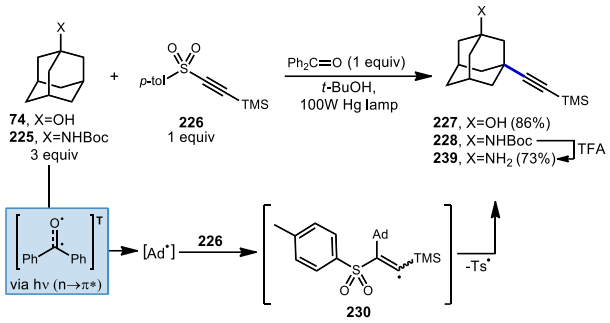

Xu and coworkers investigated an efficient method for the direct alkynylation of substrates containing unactivated C(sp^3)–H bonds under metal-free conditions using an ethynyl benziodoxolone (EBX) **231** (**Scheme 36**).[134] When adamantane was used, C–H functionalization was selective for the tertiary position and a 59% yield was reported for the adamantyl product **232**. The authors did not quantify the regioselectivity for adamantane but the same reaction with methylcyclohexane reacted at the tertiary position selectively (>25:1 r.r.). The reaction was completely suppressed by the radical trapping agent TEMPO, and the alkyl-TEMPO product was observed, suggesting the reaction proceeds via a radical intermediate. A plausible mechanism begins with thermal homolytic cleavage of DTBP to generate the *tert*-butoxyl radical, which reacts with adamantane giving the adamantyl radical. This is followed by addition to the triple bond of the EBX reagent with subsequent β-elimination to give the final alkynylated product.

Scheme 36. Adamantane Alkynylation Using EBX Reagent 231

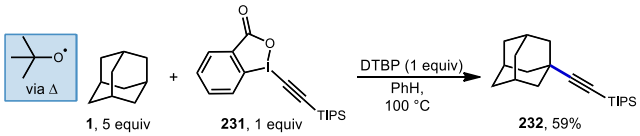

Recently, Tang and coworkers reported an alkynylation of adamantane using a pyridine-boryl radical (**Scheme 37**).[135] Using bis(neopentyl glycolato)-diboron **234**, 4-cyanopyridine is added to facilitate ligand-induced B–B homolysis to generate the key boryl radical (see **235→236**). The adamantyl radical is then produced which adds into ((phenylethynyl)sulfonyl)benzene (**233**). The resulting vinyl radical intermediate **237** then fragments with loss of sulfonyl radical to afford the alkyne product **220**. This alkynylation approach gave the final product in 62% yield with only marginal preference for the tertiary adamantyl position (3°:2°=5:4). The inclusion of 4-cyanopyridine-*N*-oxide as oxidant was needed for best results; however, control experiments using cyclohexane without the use of any oxidant still proceeded in 12% yield suggesting that oxygen may also function as an oxidant to some degree.

Scheme 37. Boryl Radical-Mediated Adamantane Alkynylation

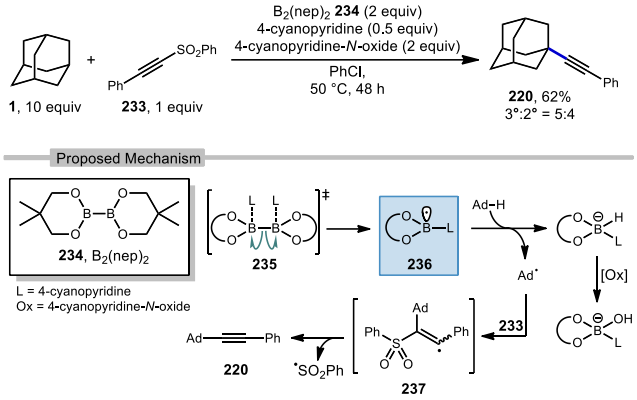

6 - Arylation

Aryl adamantanes appear both as scaffolds in nanomaterials and in bioactive compounds, such as the marketed acne medication adapalene (**5**), known by the generic name Differin. These compounds can be constructed by non-radical methods such as transition metal catalysis or by radical-mediated C–H arylation, which will be discussed here.

6.1 - *Photooxidations Using TCB*

In 1996, Albini et al. used 1,2,4,5-tetracyanobenzene (TCB) to arylate adamantane in a UV-promoted process.[136,137] The mono-arylated product **239** (**Scheme 38a**) was predominantly formed by reaction exclusively at the tertiary position while the di-arylated product **240** was formed to a lesser degree. Under UV-light, Albini had previously shown that TCB in its singlet excited state is a strong oxidant capable of inducing SET from a variety of alkanes.[138] After oxidation, a solvent-caged adamantyl radical cation/TCB radical anion pair is generated (see **241**, **Scheme 38b**). The adamantyl radical cation then either loses a proton to solvent or, in the case of a substituted adamantane, may undergo substituent elimination to create the tertiary adamantyl radical. The C–C cleavage that occurs with substituent elimination is an endergonic process while deprotonation to form the adamantyl radical is exergonic (approx. -17.1 kcal/mol) and is therefore the favored route to the adamantyl radical. After its formation, the adamantyl radical then quickly recombines with the radical anion of TCB to form anion **242** (analogous to a Meisenheimer complex) and rearomatization through the loss of cyanide then gives the arylated adamantyl product.

Scheme 38. Light-Driven Arylation of Adamantanes Using TCB

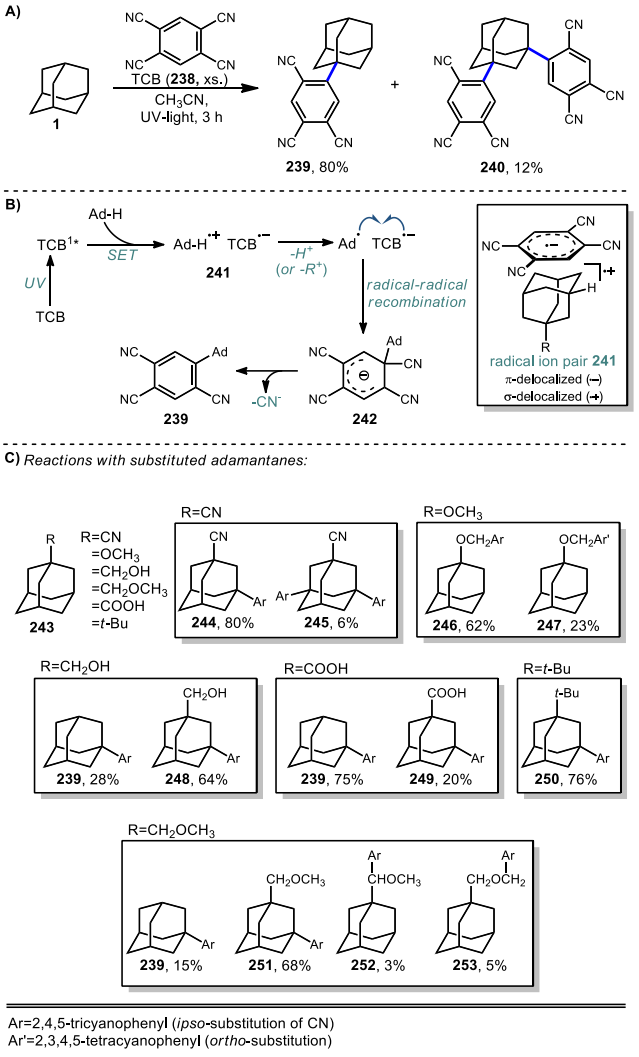

Several substituted adamantanes (**243**) were subjected to the same conditions, resulting in the formation of a variety of products formed through mono- or bis- C–H arylation of the cage, arylation with loss of the substituent, or C–H arylation of the substituent itself (**Scheme 38c**). Arylation of 1-methoxyadamantane occurred on the methoxy substituent rather than on the adamantyl moiety, giving two benzylic ether products. The expected 2,4,5-tricyanophenyl substitution product **246** was predominantly produced (63% yield) but interestingly, an appreciable amount of *ortho*-functionalization also occurred to form 2,3,5,6-tetracyanophenyl product **247** (23% yield). 1-Adamantanecarboxylic acid proceeded mostly with decarboxylation to the monoaryl adamantane product **239** with a minor amount retaining the carboxy group (**249**).

Figure 4. TCB Arylation of Higher-Order Diamondoids

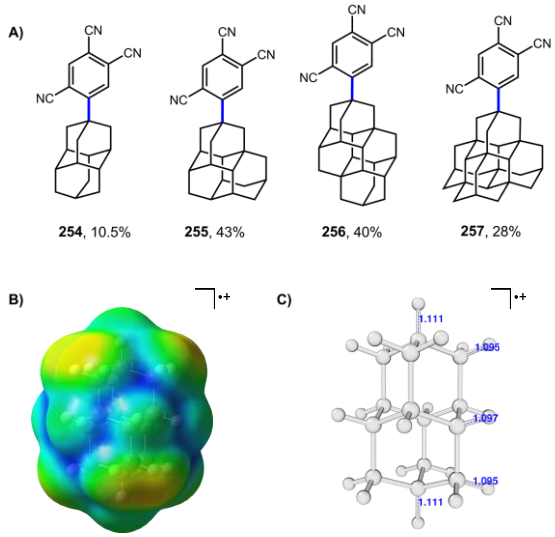

A) TCB arylation of higher order diamondoids. **B)** Electrostatic potential surfaces for the diamantyl radical cation (symmetrically σ-delocalized). **C)** C–H bond lengths (Å) for diamondoid radical cations are longest at their geometric center (apical postions). Optimized using B3LYP/6-31(d).

More recent work by Schreiner, Fokin, and coworkers showed that arylation with TCB on higher order diamondoids (**254-257**) proceeds with 100% apical selectivity (**Figure 4a**).[75,139,140] This remarkable selectivity surpasses the vast majority of reactions of higher order diamondoids such as acetylation (see **Figure 3**). Delocalization of the radical cation through the sigma framework, as represented in blue in the electrostatic potential surface in **Figure 4b**, leads to elongation and weakening of the apical C–H bonds (**Figure 4c**), which are more easily deprotonated to give apical radicals selectively. The UV-promoted arylation was demonstrated up to pentamantane with high selectivity. Virtually no functionalization reactions beyond pentamantane have been reported in the literature, perhaps due to difficulty in accessing sufficient quantities of pure starting materials.

6.2 - *Minisci-type Arylations*

Scheme 39. General Minisci-type Radical Addition

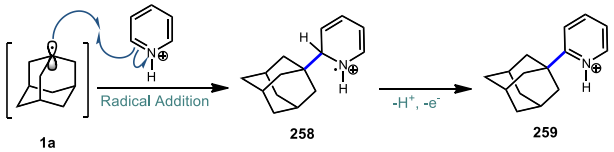

Minisci reactions like the one shown in **Scheme 39** are characterized by the addition an alkyl radical to an electron-deficient heteroaromatic compound, leading to the formation of a new C(sp^3)–C(sp^2) bond.[141] Heteroaromatic adamantane-containing nucleoside analogs have been known to possess antiherpetic[63] and antifolate[142] activity and can be synthesized using Minisci-type reactions. Traditionally these reactions have applied stoichiometric ammonium persulfate and silver nitrate to induce an oxidative decarboxylation to generate the alkyl radical.[143] This decarboxylative approach using 1-adamantanecarboxylic acid (**260**) was taken in the preparation of **262**, an adamantane containing anti-tuberculosis precursor as shown in **Scheme 40**.[144] Adamantane was also used in early work by Barton for the alkylation of caffeine **264** and other purines.[145,146] Since then, several methods have been developed that are metal-free or do not rely on pre-functionalized adamantanes to arrive at the adamantyl radical intermediate.

Scheme 40. Traditional Minisci Approaches

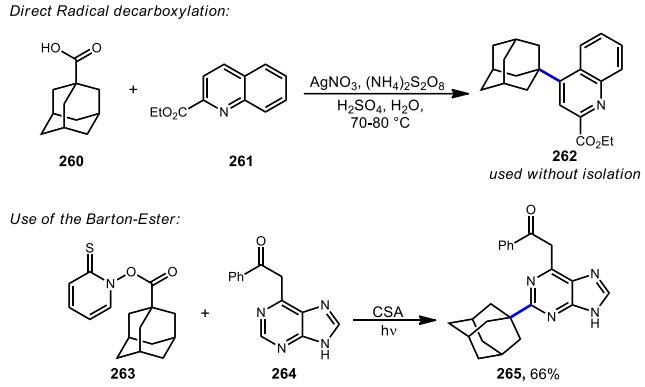

In 2013, Antonchick and coworkers developed a Minisci-type arylation reaction using a selective oxidative cross-coupling approach.[147] One example, shown in **Scheme 41**, shows the arylation of adamantane using 4,7-dichloroquinoline (**266**) in the presence of phenyliodine bis(trifluoroacetate) (PIFA) as oxidant and NaN_3, as a critical additive. The key H-atom abstractor is likely the azide radical and the corresponding arylated product **267** was obtained in 84% yield as a single isomer. Overall, Antonchick et al. used this metal-free oxidative cross-coupling approach of heteroarenes and a variety of alkanes to obtain arylated products under mild, non-acidic conditions, with short reaction times and in high yields.

Kwong et al. and Guo et al. have also shown that DTBP can enable the oxidative cross coupling of adamantane with indoles[148] (**268**→**269**) and purine nucleosides[149] (**270**→**271**) under similar reaction conditions

Scheme 41. Oxidative Minisci Arylation Using Sodium Azide

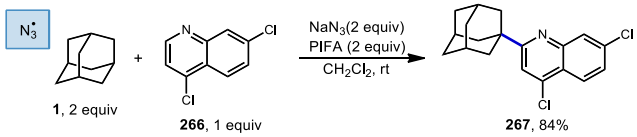

(**Scheme 42**). Both methods were developed using neat cycloalkanes or cyclic ethers, however adamantane, a solid, requires an aromatic solvent (e.g., xylene or benzene). In both cases, an excess of five equivalents of adamantane was enough for the reaction to proceed in moderate to good yield.

Scheme 42. Minisci Reactions of Indoles and Purines Using DTBP

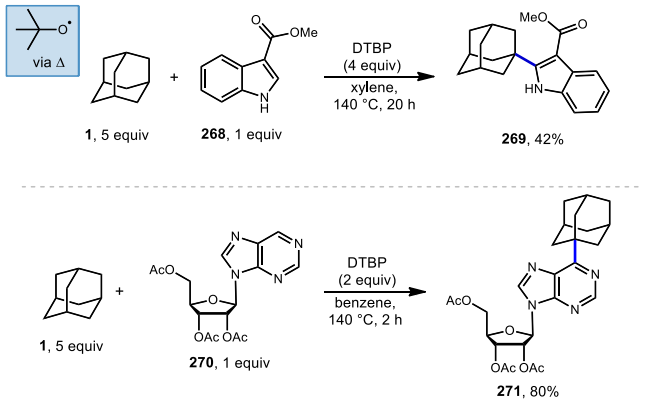

More recently in 2017, Li et al. also found the *tert*-butoxyl radical was effective for oxidative cross couplings of adamantane with oxazoles and thiazoles (**Scheme 43**).[150] The *tert*-butoxyl radical in this case does not originate from DTBP and instead comes from the homolysis of *tert*-butylperoxybenzoate (TBPB) and uses catalytic cobalt(II) chloride to assist in radical generation, presumably through the formation of a cobalt(III) benzoate. This approach afforded the both the adamantyl oxazole **273** and thiazole **274** products in moderate yield.

Scheme 43. Cobalt-Assisted Minisci Reactions of Oxazoles and Thiazoles

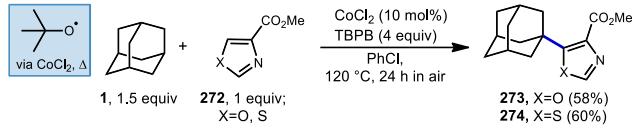

Togo et al. showed that the introduction of heteroaromatic bases onto hydrocarbons can also be accomplished using benzoyl peroxide in the absence transition metals and under irradiation free conditions.[151] When adamantane and lepidine (**275**) were treated with trifluoroacetic acid in benzene under irradiation with benzoyl peroxide, the desired alkylated quinoline product **276** was obtained in 75% yield (**Scheme 44a**). Other heteroaromatic bases also produced the arylated product in good yields (**277**-**279**; 63-86%). In this reaction, thermal homolysis of benzoyl peroxide generates benzoyloxy radical (or phenyl radical after thermal decarboxylation) which then abstracts a hydrogen from adamantane generating the adamantyl radical. Nucleophilic radical addition with a protonated heteroaromatic base and subsequent oxidation (formal loss of H-atom) forms the protonated product. Lepidine alkylation with adamantane has also been reported by Jin and coworkers using hydrogen peroxide and blue light as a source of hydroxyl radical (**Scheme 44b**).[152]

Scheme 44. Minisci Reactions Involving Lepidine (275) and Other Heteroaromatic Bases

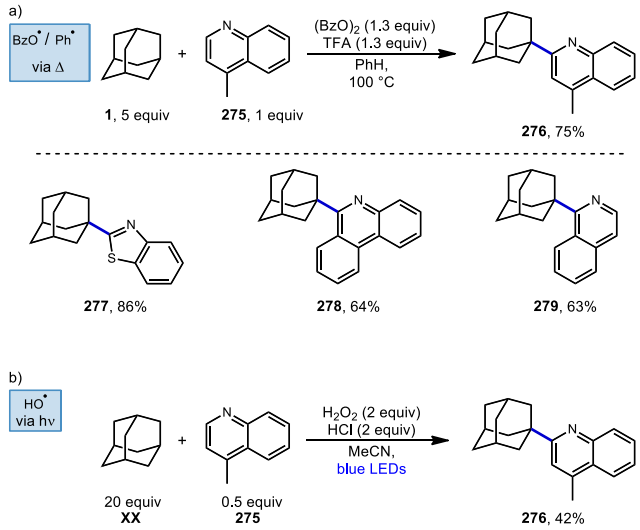

6.3 - *Dual-Catalytic Arylation*

In 2018, another direct arylation was performed by MacMillan and coworkers using a dual catalytic system of 1 mol% tetrabutylammonium decatungstate and 5 mol% nickel bipyridine complex (**Scheme 45**).[153] Adamantane derivatives underwent arylation predominantly at the methylene position for both 2-adamantanone (**75**) and bromo-adamantanone (**281**) to give a 53% and 48% yield, respectively.

Interestingly in another study, MacMillan and coworkers observed selective arylation at the methylene position of two adamantanone substrates despite existing precedent that decatungstate-catalyzed functionalization occurs in a 5:1 ratio favoring the methine position of adamantane.[154] This reversal in regioselectivity can be rationalized by the

deactivating effect of the ketone on the adjacent 3°-positions and reversible radical capture during nickel-catalysis, with the selectivity being imparted by a preference for reductive elimination of the 2° aryl adamantane product.[155] Notably, in this work, the authors report both regioselectivity and diastereoselectivity (at the new methine stereocenter) in these functionalized adamantyl products. This was achieved by careful separation of the individual regio- and stereoisomers from the crude reaction mixture.

Scheme 45. Photochemically Driven Nickel Catalysis of Adamantanones

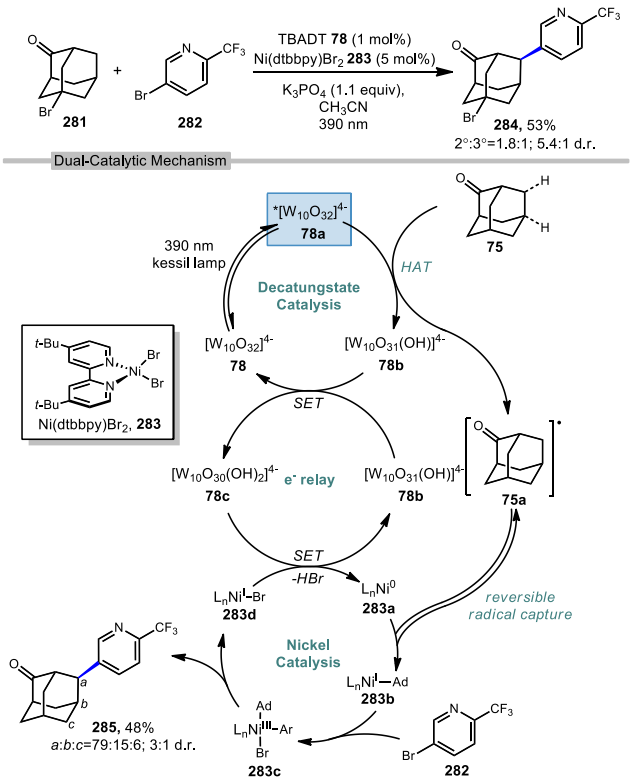

The proposed mechanism begins with the photoexcitation of TBADT followed by intersystem crossing to give the triplet excited state (**78**→**78a**). This is followed by HAT from a hydrocarbon like 2-adamantanone (**75**) by the photoexcited catalyst, providing the singly reduced decatungstate **78b** and the adamantyl radical **75a**. MacMillan proposes a disproportionation event involving the singly reduced decatungstate to regenerate the active HAT catalyst and form a doubly reduced decatungstate species **78c**. The alkyl radical is captured by Ni(0) leading to an alkyl Ni(I) intermediate (**238a**→**238b**). Oxidative addition of the aryl bromide then gives the key Ni(III) intermediate **283c** which undergoes reductive elimination to yield the desired cross-coupled aryl product **285**. A final SET step and loss of HBr between the active nickel catalyst and double-reduced TBADT catalyst complete both catalytic cycles.

6.4 - *Cascade Reactions Involving Aromatic Systems*

DTBP and copper have been used together with adamantane for accomplishing arylative transformations that occur through a radical cascade process. While an adamantyl radical is not directly involved in arylation, these reactions involve radical addition into an acceptor which triggers a subsequent proximity-induced intramolecular aromatic substitution to give arylated adamantane products.

Scheme 46. Cascade Arylations Involving Isothiocyanates

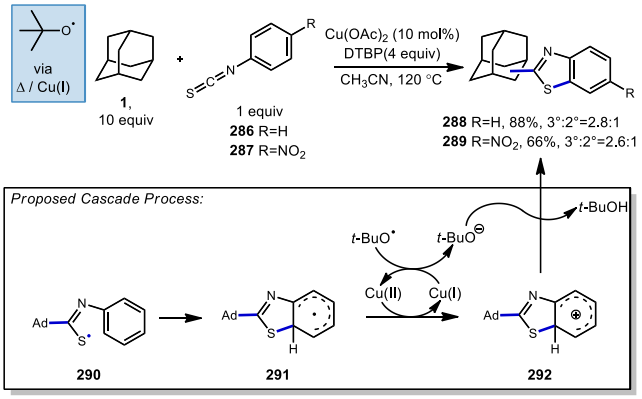

Yadev and Yadev reported the use of isothiocyanates (**286**, **287**) for the formation of adamantyl benzothiazoles (**288**, **289**) using excess DTBP and catalytic copper(II) diacetate.[156] In this process, DTBP is homolytically converted to an oxyradical through either thermal or Cu-mediated decomposition and then generates the adamantyl radical. The adamantyl radical adds into the isothiocyanate to form resonance-stabilized thiyl radical intermediate **290** and then cyclizes to the cyclohexadienyl radical **291**. Oxidation by Cu(II) or *tert*-butoxyl radical to the cyclohexadienyl cation **292** then follows and deprotonation with *tert*-butoxide gives the final benzothiazole product. The yield and distribution of 3° and 2° adamantyl products was slightly dependent on the substitution of the isothiocyanate with *para*-nitro derivative **289** leading to lower yield and regioselectivity.

Scheme 47. Copper-Catalyzed Annulation Involving Aryl Isocyanides

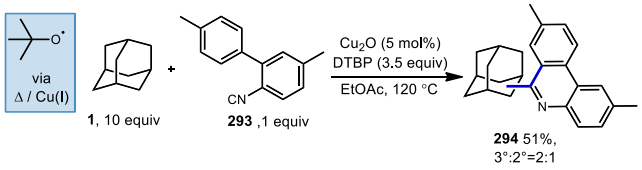

Similarly, Zhu et al. demonstrated a related cascade process under similar copper-catalyzed conditions using aryl isocyanides (**Scheme 47**).[157] Adamantane was used with 2-isocyanobiphenyl **293** to form a 2:1 mixture of adamantyl phenanthridines **294** in 51% yield. This powerful transformation enables dual C–C bond formation to the isocyanide carbon using both C(sp^3)–H and C(sp^2)–H functionalizations.

Li and coworkers reported another cascade with adamantane using *N*-methyl-*N*-phenylmethylacrylamide (**295**, **Scheme 48**) with Cu_2O and dicumyl peroxide (DCP) to afford cyclized 3,3-dialkyloxindole **296** in 68% yield and a 6:1 ratio favoring the tertiary adamantyl position.[158] The

Scheme 48. Cascade Annulation of Adamantanes Involving Cu(II) and Peroxide

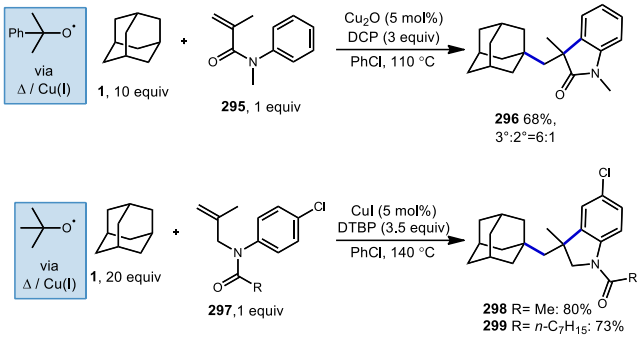

mechanism of this reaction begins with a Giese-type addition to the alkene, followed by cyclization and rearomatization analogous to the mechanism in **Scheme 46**. DCP was chosen over DTBP by the authors due to better results with it during optimization using cyclohexane. A similar cascade process using DTBP has been reported by Liang et al. with *N*-allylanilides **297** to give 3,3-dialkyl-indolines **298** and **299** selectively at the tertiary adamantyl position.[159]

7 - Introduction of Nitrogen-Containing Groups

7.1 - *Cyanation*

Classically, cyanation reactions are usually thought of in terms of the nucleophilic character of simple cyanides such as KCN adding to an electrophilic reaction partner. However, over the years, a variety of electrophilic cyanation reagents have been developed[160] and pair well with the nucleophilic character of the adamantyl radical.

Inoue and coworkers showed that using benzophenone as a photomediator in conjunction with *p*-toluenesulfonyl cyanide (**300**, TsCN), adamantane and adamantanol could be cyanated in high yield (**Scheme 49**).[161,162] Both cyanoadamantane products **301** and **302** were obtained as the methine addition products. In this reaction, the oxyl radical generated from excitation of benzophenone abstracts a hydrogen from the tertiary position on adamantane giving an adamantyl radical. This nucleophilic radical then goes on to react with TsCN generating the product and a sulfinyl radical. Catalytic turnover occurs with HAT by the sulfiniyl radical from the ketyl intermediate giving sulfinic acid and the renewed photocatalyst. Although benzophenone was used stoichiometrically with adamantane, the reaction proceeded when used in substoichiometric quantities with other substrates such as 1,2-dioxane.

Scheme 49. Benzophenone-Mediated Cyanation of Adamantanes

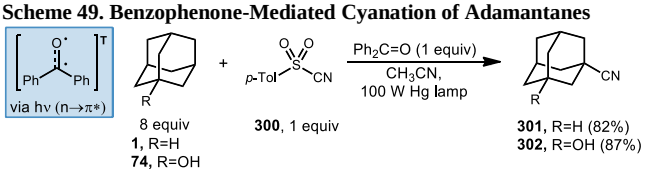

Schreiner et al. have also found that using TsCN as an electrophilic cyanide source with a NHPI/PINO system effectively cyanated a variety of adamantanes and diamantanes (**Scheme 50**).[163] A few known reaction conditions were tried in order to access the PINO radical such as azobisisobutyronitrile (AIBN), Co(II/III) salts, and ceric ammonium nitrate (CAN). CAN was found to be superior in this regard, and initially gave the 1-cyanoadamantane product **301** in 42% yield. However, the formation of significant amounts of 1-nitroadamantane as a side product was also observed with the use of CAN. The addition of base suppressed the formation of the undesired nitro product with lithium carbonate giving the best result. Under this optimized TsCN/NHPI/CAN/Li_2CO_3 system, the cyanoadamantane was obtained in 77% yield. Other substituted adamantanes were obtained with varying degrees of success (**303-314**). Methyl adamantane **303** was obtained 71% yield, while di- and trimethyl adamantanes **307** and **308** were only isolated with yields of 33% and 28%, respectively. This drop in reactivity was also observed by Olah and coworkers in the cyanations of methylated bromoadamantanes using Lewis acid catalysis.[164]

A range of other useful adamantyl nitriles were accessible including acetamides, phthalimides, azides, alkynes, and silyl ethers. Diamantane **315** was also cyanated in a 4.3:1 ratio favoring the medial position, while the carboxylate derivative **316** was was formed as a mixture of medial regioisomers (1.1:1 r.r.). Notable among these reaction conditions is the use of only one equivalent of adamantane. Typically, most adamantane C–H activation reactions will use higher amounts of the adamantane in order to suppress further C–H activation of the product. Here, however, installation of the electron withdrawing cyano group deactivates the cage to further cyanation, as evidenced by the difference in yield between the formation of mono- and di-cyanated products **301** and **306**.

Scheme 50. HAT-Mediated Cynation of Diamondoids via PINO Radical

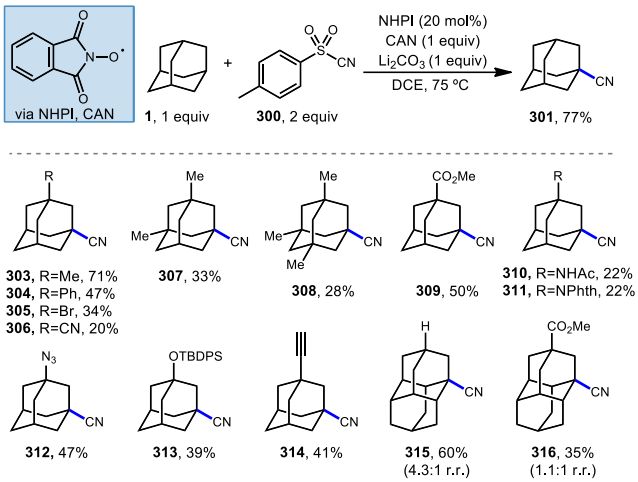

In 2018 Ma, Zhang and coworkers reported a metal-free cyanation reaction using a hypervalent iodine reagent (**317**, **Scheme 51**).[165] With 20 mol% of TBPB as a catalytic initiator, C(sp^3)–H bonds in a very broad scope of cyclic hydrocarbons, ethers and amine derivatives underwent direct cyanation at elevated temperature, including adamantane in 76% yield as determined by ^{1}H NMR. The initial HAT occurs with the *tert*-butoxyl or phenyl radical (formed through decarboxylation of the benzoyloxy radical), while the chain-carrying radical is likely the aroyloxy radical derived from 2-iodobenzoic acid. Spin-trapping and competition experiments were consistent with a radical mechanism for hydrocarbons and iminium ion generation with amine substrates.

Scheme 51. Cyanation of Adamantane Using Hypervalent Iodine

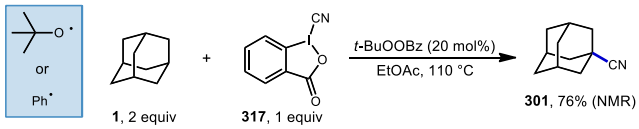

7.2 - *Aminoalkylation*

DTBP was also used for the α-alkylation of α-amino carbonyls **318** with adamantane and other alkanes by Cheng et al. (**Scheme 52**).[166] The *tert*-butoxyl radical is thought to both facilitate the formation of the imine intermediate **318a** and generate the adamantyl radical that adds into the

imine, necessitating the use of excess peroxide. Aminoalkylated product **319** was isolated in 46% yield as the tertiary regioisomer.

Scheme 52. Aminoalkylation of Adamantane Using DTBP

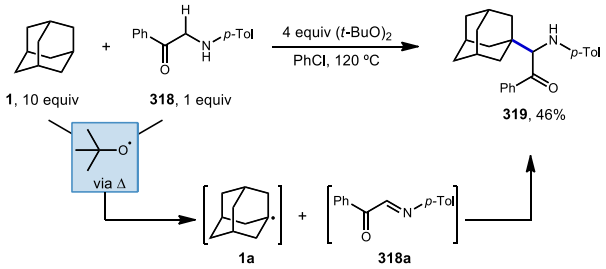

In 2020, our group described an aminoalkylation strategy with adamantanes using a dual photocatalytic/HAT system (described earlier in Section 4.2).[167] A variety of protected imines and hydrazones were used as radical acceptors to generate aminoadamantyl products (**Scheme 53)** in moderate to high yields with excellent selectivity for tertiary adamantyl position. Electron-deficient hydrazones **320-322** and *N*-tosylimines **323-325** with electron-withdrawing aryl groups (Y=CO_2Me, CN, F) worked better than those bearing neutral or donating groups (Y=H, OMe). A trisubstituted cyclic sulfonylimine demonstrated this reaction's ability to form even the sterically congested C–C bond in sulfonamide product **326** in 83% yield. This cyclic sulfonylimine also reacted well with substituted adamantanes **327-329** such as 1-adamantanol, although other electron-withdrawing substituents (R^2=Cl, Ac) were less effective.

Scheme 53. Aminoalkylation of Adamantanes via Dual Photoredox/HAT Catalysis

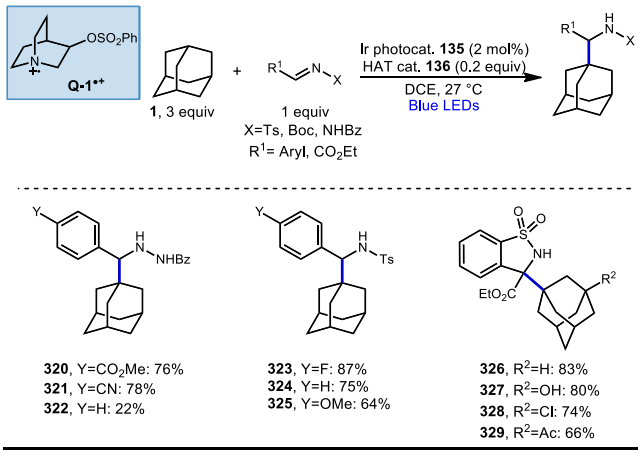

The use of the *N*-mesitylsulfinyl group as a chiral auxiliary provided good stereocontrol for the radical addition of adamantane to sulfinimine substrate **330** (X=Mes, Y=Ph) and the sulfinamide product **331** was obtained in 73% yield and >20:1 d.r. (**Scheme 54**). Other sulfinyl groups such as *tert*-butyl and *para*-tolyl were less effective at asymmetric induction than the mesityl group (see reactions with glyoxalate-derived sulfinimines **332-334**). In contrast to the protected imines in **Scheme 53**, the chiral sulfinimines performed better using PT catalyst **187** (see **Scheme 30**) as the direct HAT photocatalyst, which still displayed excellent regioselectivity and resulted in less degradation of the starting material under the reaction conditions.

Deprotection of the aminoalkylated products to their free amines with SmI_2 or TFA leads to useful drug-like pharmacophores and building blocks. In particular r, after deprotection of the sulfinyl group, glyoxylate-derived chiral sulfinimines enabled direct preparation of an enantiopure adamantyl glycine from **334** and the 3-hydroxyadamantyl core of saxagliptin from precursor **335**.

Scheme 54. Asymmetric Aminoalkylation of Adamantanes

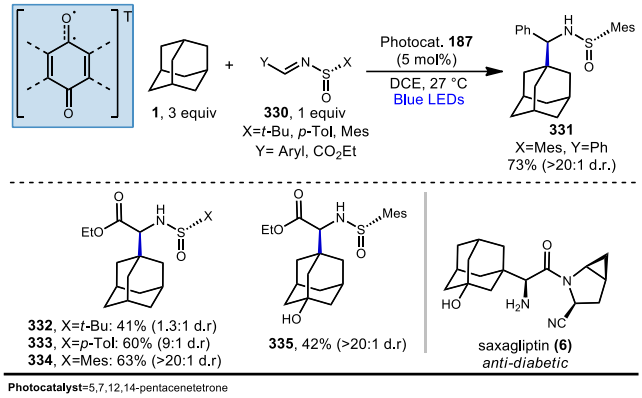

8 - Summary and Outlook

Figure 5. Summary of regioselectivity profiles for the most common H-atom abstractors

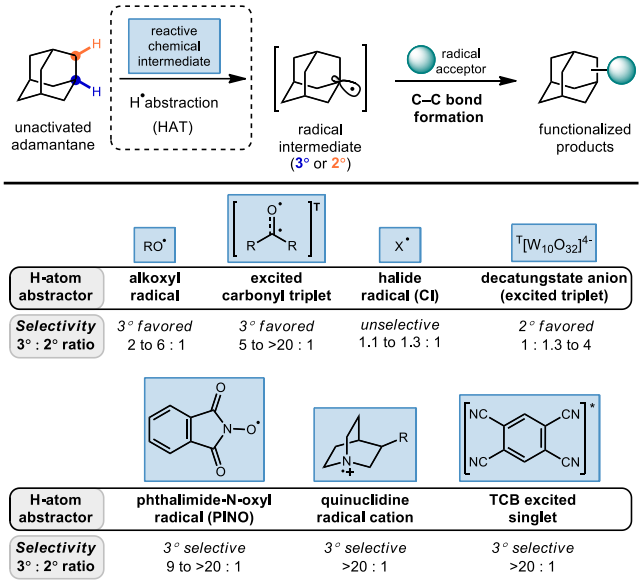

The functionalization of adamantanes and higher diamondoids has garnered continued interest from the late 1950s when they became readily available to the present day. As part of this sustained effort, adamantanes have served as test substrates for a variety of C–H functionalization reactions, particularly due to the unusually strong C(sp^3)–H bonds, providing a challenging molecule in terms of both reactivity and regioselectivity. Furthermore, derivatized adamantanes have served as important synthetic targets in their own right, particularly due to their versatile use as architectural linkers and as a "lipophilic bullet" in medicinal chemistry applications, as it was described by Schreiner and coworkers.[10] Beginning with the early work of Schleyer and Haaf, increased access to adamantane derivatives has driven new discoveries in biological and chemical function, and new applications have in turn offered the motivation for more versatile synthetic methods. This interest in diamondoids within synthesis and catalysis disciplines continues to reinforce the need for novel regioselective methods.

As we have summarized in this Review, key to the selectivity between different C–H bonds in the context of radical reactions is the

nature of the H-atom abstracting species (**Figure 5**). Upon examining the many reactions described above, certain trends become apparent. For adamantane itself, selectivity for the sterically more accessible 3º-C–H bond over the 2º-position ranges from >20:1 in case of the quinuclidine-derived radical cation **X,** the PINO radical, and photoexcited TCB (via oxidation/deprotonation mechanism) to approximately 2-5:1 in the case of various examples of *tert*-butoxyl radical-mediated reactions, to ~1:1.3 in the case of decatungstate as reported by Albini and Ryu. The range for HAT using an excited carbonyl triplet (i.e., benzophenone, diacetyl, quinones) also favors the 3º-position but varies considerably between medium to high selectivity based on the abstractor and reaction conditions used. With 2-adamantanone substrates, the selectivity of decatungstate reported by MacMillan and coworkers shifted further up to 1:4, favoring the 2º position, which is at least in part due to a proposed reversible activation process followed by a selective product-forming reductive elimination from nickel. Evidently, the inherent selectivity of each abstracting species can be estimated, but varies from reaction to reaction based on the nature of the next C–C (or C–X) bond-forming step and whether the key C–H abstracting step is reversible. Furthermore, some reports do not quantify any minor products, so one cannot conclusively determine a regioisomeric ratio in these cases. These factors complicate a rigid assignment of selectivity for each species, but lead to the ranges shown in **Figure 5**. The pioneering work of Schreiner and colleagues has provided a detailed look into the regioselectivity of many different processes (some of which are outside the scope of this review, i.e., C–X bond formation), including comparing experimental C1:C2 ratios to calculated transition state energies and similar comparisons for kinetic isotope effect experiments.

A full description of regioselectivity with higher order diamondoids is similarly complicated by limited data, particularly the small number of reports of functionalizations beyond diamantane. In general, the 3º-positions react preferentially, but the ratio between apical and medial positions varies based on the abstracting species. Schreiner and Fokin have reported the regioselective acetylation of diamantane with 4.6:1 selectivity for the apical position (see section 2.2). Similar apical selectivity observed across several tri- to pentamantane substrates points to polarizability in the C–H abstraction step with triplet diacetyl being the most important contributor. The photochemical arylation described by Albini through an oxidation/deprotonation mechanism with TCB was applied to diamantane, which also resulted in selective apical functionalization (11% yield, single isomer), and impressively, Schreiner and Fokin demonstrated this apical selectivity applies to even higher-ordered diamondoids. This outcome is predicted based on elongation (and acidification) of the apical C–H bonds in the radical cation that results from photooxidation. Schreiner has also calculated barriers for C1, C3 and C4-functionalizations of diamantane with different activation reagents, further highlighting the role of polarizability and other factors in the apical-selective acetylation and charge-transfer effects in medial-selective PINO-catalyzed substitutions. For a longer description of the selective functionalization of diamantane in other C–H to C–X transformations not covered here, the work of Schreiner and Fokin should be highlighted.[140]

In the larger context of C–H activation chemistry, documenting the role of the effects described above can allow a better understanding of existing methods and inspire the design of new C–H functionalization systems. The unusual properties of adamantane and diamantane allow us to probe the dominant factor for selectivity in each case, distinguishing between sterics, charge-transfer effects and polarizability. These insights may guide not only the selection of appropriate methods for a given diamondoid target, but also the application of these methods to other substrate classes beyond the diamondoids. Given the continued use of adamantanes as linkers in nanomaterials, as “lipophilic bullets” in the optimization of therapeutics and as bulky, electron-rich substituents in a variety of ligand-design applications, we expect that interest in the new methods for the selective functionalization of diamondoids will continue to attract the attention and innovative minds of organic chemists for the foreseeable future.

9 - References

1 R. C. Fort, *Adamantane: The Chemistry of Diamond Molecules*, Marcel Dekker, New York, 1976, vol. 5.
2 H. Schwertfeger, A. A. Fokin and P. R. Schreiner, *Angew. Chem. Int. Ed.*, 2008, **47**, 1022.
3 J. E. P. Dahl, J. M. Moldowan, T. M. Peakman, J. C. Clardy, E. Lobkovsky, M. M. Olmstead, P. W. May, T. J. Davis, J. W. Steeds, K. E. Peters, A. Pepper, A. Ekuan and R. M. K. Carlson, *Angew. Chem. Int. Ed.*, 2003, **42**, 2040.
4 H.-C. Chang, *J. Phys. Conf. Ser.*, 2016, **728**, 062004.
5 C. Tyborski, T. Hückstaedt, R. Gillen, T. Otto, N. A. Fokina, A. A. Fokin, P. R. Schreiner and J. Maultzsch, *Carbon*, 2020, **157**, 201.
6 T. Rander, T. Bischoff, A. Knecht, D. Wolter, R. Richter, A. Merli and T. Möller, *J. Am. Chem. Soc.*, 2017, **139**, 11132.
7 M. Vörös, T. Demjén, T. Szilvási and A. Gali, *Phys. Rev. Lett.*, 2012, **108**, 267401.
8 A. Milanese, E. Gorincioi, M. Rajabi, G. Vistoli and E. Santaniello, *Bioorganic Chem.*, 2011, **39**, 151.
9 D. J. Augeri, J. A. Robl, D. A. Betebenner, D. R. Magnin, A. Khanna, J. G. Robertson, A. Wang, L. M. Simpkins, P. Taunk, Q. Huang, S.-P. Han, B. Abboa-Offei, M. Cap, L. Xin, L. Tao, E. Tozzo, G. E. Welzel, D. M. Egan, J. Marcinkeviciene, S. Y. Chang, S. A. Biller, M. S. Kirby, R. A. Parker and L. G. Hamann, *J. Med. Chem.*, 2005, **48**, 5025.
10 L. Wanka, K. Iqbal and P. R. Schreiner, *Chem. Rev.*, 2013, **113**, 3516.
11 T. P. Stockdale and C. M. Williams, *Chem. Soc. Rev.*, 2015, **44**, 7737.
12 J. Joubert, W. J. Geldenhuys, C. J. Van der Schyf, D. W. Oliver, H. G. Kruger, T. Govender and S. F. Malan, *ChemMedChem*, 2012, **7**, 375.
13 J. G. Henkel, J. T. Hane and G. Gianutsos, *J. Med. Chem.*, 1982, **25**, 51.
14 K. A. Agnew-Francis and C. M. Williams, *Adv. Synth. Catal.*, 2016, **358**, 675.
15 A. J. Arduengo, R. L. Harlow and M. Kline, *J. Am. Chem. Soc.*, 1991, **113**, 361.
16 A. G. Dossetter, T. F. Jamison and E. N. Jacobsen, *Angew. Chem. Int. Ed.*, 1999, **38**, 2398.
17 B. K. Keitz, K. Endo, P. R. Patel, M. B. Herbert and R. H. Grubbs, *J. Am. Chem. Soc.*, 2012, **134**, 693.
18 R. P. Reddy, G. H. Lee and H. M. L. Davies, *Org. Lett.*, 2006, **8**, 3437.
19 Q. Li, C. Jin, P. A. Petukhov, A. V. Rukavishnikov, T. O. Zaikova, A. Phadke, D. H. LaMunyon, M. D. Lee and J. F. W. Keana, *J. Org. Chem.*, 2004, **69**, 1010.
20 Q. Li, A. V. Rukavishnikov, P. A. Petukhov, T. O. Zaikova, C. Jin and J. F. W. Keana, *J. Org. Chem.*, 2003, **68**, 4862.
21 K. Nasr, N. Pannier, J. V. Frangioni and W. Maison, *J. Org. Chem.*, 2008, **73**, 1056.
22 O. Plietzsch, C. I. Schilling, M. Tolev, M. Nieger, C. Richert, T. Muller and S. Bräse, *Org. Biomol. Chem.*, 2009, **7**, 4734.
23 H. Lim and J. Y. Chang, *Macromolecules*, 2010, **43**, 6943.
24 Q. Fang, S. Gu, J. Zheng, Z. Zhuang, S. Qiu and Y. Yan, *Angew. Chem. Int. Ed.*, 2014, **53**, 2878.
25 Q. Fang, J. Wang, S. Gu, R. B. Kaspar, Z. Zhuang, J. Zheng, H. Guo, S. Qiu and Y. Yan, *J. Am. Chem. Soc.*, 2015, **137**, 8352.
26 P. Kahl, J. P. Wagner, C. Balestrieri, J. Becker, H. Hausmann, G. J. Bodwell and P. R. Schreiner, *Angew. Chem. Int. Ed.*, 2016, **55**, 9277.
27 H. Decker, *Angew. Chem.*, 1924, **37**, 781.
28 S. Landa and V. Macháček, *Collect. Czechoslov. Chem. Commun.*, 1933, **5**, 1.
29 V. Prelog and R. Seiwerth, *Berichte Dtsch. Chem. Ges. B Ser.*, 1941, **74**, 1644.
30 V. Prelog and R. Seiwerth, *Berichte Dtsch. Chem. Ges. B Ser.*, 1941, **74**, 1769.

31 H. Meerwein, F. Kiel, G. Klösgen and E. Schoch, *J. Für Prakt. Chem.*, 1922, **104**, 161.
32 R. C. Fort and P. von R. Schleyer, *Chem. Rev.*, 1964, **64**, 277.
33 H. Stetter, O.-E. Bänder and W. Neumann, *Chem. Ber.*, 1956, **89**, 1922.
34 P. von R. Schleyer, *J. Am. Chem. Soc.*, 1957, **79**, 3292.
35 P. von R. Schleyer and M. M. Donaldson, *J. Am. Chem. Soc.*, 1960, **82**, 4645.
36 P. von Ragué Schleyer, P. Grubmüller, W. F. Maier, O. Vostrowsky, L. Skattebøl and K. H. Holm, *Tetrahedron Lett.*, 1980, **21**, 921.
37 M. A. McKervey, *Chem. Soc. Rev.*, 1974, **3**, 479.
38 R. P. Kirchen, T. S. Sorensen and S. M. Whitworth, *Can. J. Chem.*, 1993, **71**, 2016.
39 C. Cupas, P. von R. Schleyer and D. J. Trecker, *J. Am. Chem. Soc.*, 1965, **87**, 917.
40 T. M. Gund, E. Osawa, V. Z. Williams and P. V. R. Schleyer, *J. Org. Chem.*, 1974, **39**, 2979.
41 O. Farooq, S. M. F. Farnia, M. Stephenson and G. A. Olah, *J. Org. Chem.*, 1988, **53**, 2840.
42 G. A. Olah, G. K. S. Prakash, J. G. Shih, V. V. Krishnamurthy, G. D. Mateescu, G. Liang, G. Sipos, V. Buss, T. M. Gund and P. v. R. Schleyer, *J. Am. Chem. Soc.*, 1985, **107**, 2764.
43 M. A. Mckervey, *Tetrahedron*, 1980, **36**, 971.
44 J. E. Dahl, S. G. Liu and R. M. K. Carlson, *Science*, 2003, **299**, 96.
45 J. E. P. Dahl, J. M. Moldowan, Z. Wei, P. A. Lipton, P. Denisevich, R. Gat, S. Liu, P. R. Schreiner and R. M. K. Carlson, *Angew. Chem. Int. Ed.*, 2010, **49**, 9881.
46 W. Haaf, *Angew. Chem.*, 1961, **73**, 144.
47 W. Haaf, *Chem. Ber.*, 1964, **97**, 3234.
48 W. L. Davies, R. R. Grunert, R. F. Haff, J. W. McGahen, E. M. Neumayer, M. Paulshock, J. C. Watts, T. R. Wood, E. C. Hermann and C. E. Hoffmann, *Science*, 1964, **144**, 862.
49 G. Hubsher, M. Haider and M. S. Okun, *Neurology*, 2012, **78**, 1096.
50 A. Witt, N. Macdonald and P. Kirkpatrick, *Nat. Rev. Drug Discov.*, 2004, **3**, 109.
51 S. K. Sonkusare, C. L. Kaul and P. Ramarao, *Pharmacol. Res.*, 2005, **51**, 1.
52 H. Baldwin, G. Webster, L. Stein Gold, V. Callender, F. E. Cook-Bolden and E. Guenin, *Am. J. Clin. Dermatol.*, 2021, **22**, 315.
53 P. R. Schreiner, O. Lauenstein, I. V. Kolomitsyn, S. Nadi and A. A. Fokin, *Angew. Chem. Int. Ed.*, 1998, **37**, 1895.
54 P. R. Schreiner, O. Lauenstein, E. D. Butova, P. A. Gunchenko, I. V. Kolomitsin, A. Wittkopp, G. Feder and A. A. Fokin, *Chem. – Eur. J.*, 2001, **7**, 4996.
55 G. H. Kruppa and J. L. Beauchamp, *J. Am. Chem. Soc.*, 1986, **108**, 2162.
56 A. A. Fokin and P. R. Schreiner, *Chem. Rev.*, 2002, **102**, 1551.
57 Y. Ando and K. Suzuki, *Chem. – Eur. J.*, 2018, **24**, 15955.
58 R. I. Khusnutdinov and N. A. Shchadneva, *Russ. Chem. Rev.*, 2019, **88**, 800.
59 M.-G. A. Shvekhgeimer, *Russ. Chem. Rev.*, 1996, **65**, 555.
60 E. I. Bagrii, A. I. Nekhaev and A. L. Maksimov, *Pet. Chem.*, 2017, **57**, 183.
61 L. I. Kas'yan and V. A. Pal'chikov, *Russ. J. Org. Chem.*, 2010, **46**, 1.
62 M. A. Gunawan, J.-C. Hierso, D. Poinsot, A. A. Fokin, N. A. Fokina, B. A. Tkachenko and P. R. Schreiner, *New J. Chem.*, 2013, **38**, 28.
63 E. A. Shokova and V. V. Kovalev, *Russ. J. Org. Chem.*, 2012, **48**, 1007.
64 R. Hrdina, *Synthesis*, 2019, **51**, 629.
65 V. V. Sevost'yanova, M. M. Krayushkin and A. G. Yurchenko, *Russ. Chem. Rev.*, 1970, **39**, 817.
66 I. K. Moiseev, N. V. Makarova and M. N. Zemtsova, *Russ. Chem. Rev.*, 1999, **68**, 1001.
67 I. Tabushi, J. Hamuro and R. Oda, *J. Org. Chem.*, 1968, **33**, 2108.
68 G. W. Smith and H. D. Williams, *J. Org. Chem.*, 1961, **26**, 2207.
69 I. Tabushi, T. Okada, Y. Aoyama and R. Oda, *Tetrahedron Lett.*, 1969, **10**, 4069.
70 P. H. Owens, G. J. Gleicher and L. M. Smith, *J. Am. Chem. Soc.*, 1968, **90**, 4122.
71 I. Tabushi, S. Kojo and Z. Yoshida, *Tetrahedron Lett.*, 1973, **14**, 2329.
72 I. Tabushi, S. Kojo and K. Fukunishi, *J. Org. Chem.*, 1978, **43**, 2370.
73 K. Sandros and H. L. J. Bäckström, *Acta Chem. Scand.*, 1962, **16**, 958.
74 I. Tabushi, S. Kojo, P. v R. Schleyer and T. M. Gund, *J. Chem. Soc. Chem. Commun.*, 1974, 591.
75 P. R. Schreiner, N. A. Fokina, B. A. Tkachenko, H. Hausmann, M. Serafin, J. E. P. Dahl, S. Liu, R. M. K. Carlson and A. A. Fokin, *J. Org. Chem.*, 2006, **71**, 6709.
76 A. A. Fokin, P. A. Gunchenko, A. A. Novikovsky, T. E. Shubina, B. V. Chernyaev, J. E. P. Dahl, R. M. K. Carlson, A. G. Yurchenko and P. R. Schreiner, *Eur. J. Org. Chem.*, 2009, **2009**, 5153.
77 S. Kamijo, G. Takao, K. Kamijo, M. Hirota, K. Tao and T. Murafuji, *Angew. Chem. Int. Ed.*, 2016, **55**, 9695.
78 L. K. G. Ackerman, J. I. M. Alvarado and A. G. Doyle, *J. Am. Chem. Soc.*, , DOI:10.1021/jacs.8b09191.
79 H. Yuan, Z. Liu, Y. Shen, H. Zhao, C. Li, X. Jia and J. Li, *Adv. Synth. Catal.*, 2019, **361**, 2009.
80 D. H. R. Barton and D. Doller, *Acc. Chem. Res.*, 1992, **25**, 504.
81 J. Sommer and J. Bukala, *Acc. Chem. Res.*, 1993, **26**, 370.
82 B. A. Arndtsen, R. G. Bergman, T. A. Mobley and T. H. Peterson, *Acc. Chem. Res.*, 1995, **28**, 154.
83 S. Kato, T. Iwahama, S. Sakaguchi and Y. Ishii, *J. Org. Chem.*, 1998, **63**, 222.
84 I. Ryu, A. Tani, T. Fukuyama, D. Ravelli, M. Fagnoni and A. Albini, *Angew. Chem. Int. Ed.*, 2011, **50**, 1869.
85 Q. Liu, H. Zhang and A. Lei, *Angew. Chem. Int. Ed.*, 2011, **50**, 10788.
86 X.-F. Wu and H. Neumann, *ChemCatChem*, 2012, **4**, 447.
87 X.-F. Wu, H. Neumann and M. Beller, *Chem. Rev.*, 2013, **113**, 1.
88 S. E. Allen, R. R. Walvoord, R. Padilla-Salinas and M. C. Kozlowski, *Chem. Rev.*, 2013, **113**, 6234.
89 Y. Li, K. Dong, F. Zhu, Z. Wang and X.-F. Wu, *Angew. Chem. Int. Ed.*, 2016, **55**, 7227.
90 L. C. M. Castro and N. Chatani, *Chem. Lett.*, 2015, **44**, 410.
91 Z. Han, D. Chaowei, L. Lice, M. Hongfei, B. Hongzhong and L. Yufeng, *Tetrahedron*, 2018, **74**, 3712.
92 L. Lu, R. Shi, L. Liu, J. Yan, F. Lu and A. Lei, *Chem. – Eur. J.*, 2016, **22**, 14484.
93 L. Lu, D. Cheng, Y. Zhan, R. Shi, C.-W. Chiang and A. Lei, *Chem. Commun.*, 2017, **53**, 6852.
94 P. V. R. Schleyer, E. Osawa and Z. Majerski, *J. Org. Chem.*, 1971, **36**, 205.
95 United States, US3437701A, 1969.
96 I. Tabushi and K. Fukunishi, *J. Org. Chem.*, 1974, **39**, 3748.
97 K. Fukunishi and I. Tabushi, *Synthesis*, 1988, **1988**, 826.
98 A. M. González-Cameno, M. Mella, M. Fagnoni and A. Albini, *J. Org. Chem.*, 2000, **65**, 297.
99 K. Ogura, A. Kayano, N. Sumitani, M. Akazome and M. Fujita, *J. Org. Chem.*, 1995, **60**, 1106.
100 B. Wladislaw, L. Marzorati and R. B. Uchôa, *Synthesis*, 1986, **1986**, 964.
101 G. Campari, M. Fagnoni, M. Mella and A. Albini, *Tetrahedron Asymmetry*, 2000, **11**, 1891.
102 P. J. Scheuer, *Acc. Chem. Res.*, 1992, **25**, 433.
103 D. P. Curran and S. Hadida, *J. Am. Chem. Soc.*, 1996, **118**, 2531.
104 H. I. Tashtoush and R. Sustmann, *Chem. Ber.*, 1992, **125**, 287.
105 A. M. Cardarelli, M. Fagnoni, M. Mella and A. Albini, *J. Org. Chem.*, 2001, **66**, 7320.
106 L. Cermenati, D. Dondi, M. Fagnoni and A. Albini, *Tetrahedron*, 2003, **59**, 6409.
107 D. Dondi, A. M. Cardarelli, M. Fagnoni and A. Albini, *Tetrahedron*, 2006, **62**, 5527.
108 A. L. J. Beckwith and J. S. Poole, *J. Am. Chem. Soc.*, 2002, **124**, 9489.
109 H.-B. Yang, A. Feceu and D. B. C. Martin, *ACS Catal.*, 2019, **9**, 5708.
110 J. L. Jeffrey, J. A. Terrett and D. W. C. MacMillan, *Science*, 2015, **349**, 1532.

111 W.-Z. Liu and F. G. Bordwell, *J. Org. Chem.*, 1996, **61**, 4778.
112 S. Rohe, A. O. Morris, T. McCallum and L. Barriault, *Angew. Chem. Int. Ed.*, 2018, **57**, 15664.
113 K. A. Margrey, W. L. Czaplyski, D. A. Nicewicz and E. J. Alexanian, *J. Am. Chem. Soc.*, 2018, **140**, 4213.
114 C. M. Morton, Q. Zhu, H. Ripberger, L. Troian-Gautier, Z. S. D. Toa, R. R. Knowles and E. J. Alexanian, *J. Am. Chem. Soc.*, , DOI:10.1021/jacs.9b06834.
115 T. Hara, T. Iwahama, S. Sakaguchi and Y. Ishii, *J. Org. Chem.*, 2001, **66**, 6425.
116 Y. Cai, H.-S. Dang and B. P. Roberts, *Tetrahedron Lett.*, 2004, **45**, 4405.
117 A. Studer and D. P. Curran, *Angew. Chem. Int. Ed.*, 2016, **55**, 58.
118 Z.-Z. Zhang, B. Liu, C.-Y. Wang and B.-F. Shi, *Org. Lett.*, 2015, **17**, 4094.
119 W. Liu, Z. Chen, L. Li, H. Wang and C.-J. Li, *Chem. – Eur. J.*, 2016, **22**, 5888.
120 J. Ji, P. Liu and P. Sun, *Chem. Commun.*, 2015, **51**, 7546.
121 S. Kamijo, K. Kamijo, K. Maruoka and T. Murafuji, *Org. Lett.*, 2016, **18**, 6516.
122 M. W. Forkner, L. L. Miller and S. F. Rak, *Synth. Met.*, 1990, **36**, 65.
123 J. E. Almlof, M. W. Feyereisen, T. H. Jozefiak and L. L. Miller, *J. Am. Chem. Soc.*, 1990, **112**, 1206.
124 I. Baxter, D. W. Cameron and R. B. Titman, *J. Chem. Soc. C Org.*, 1971, 1253.
125 K. Wu, L. Wang, S. Colón-Rodríguez, G.-U. Flechsig and T. Wang, *Angew. Chem. Int. Ed.*, 2019, **58**, 1774.
126 M. E. Wolff, *Chem. Rev.*, 1963, **63**, 55.
127 Y. Amaoka, M. Nagatomo, M. Watanabe, K. Tao, S. Kamijo and M. Inoue, *Chem. Sci.*, 2014, **5**, 4339.
128 V. Malatesta and K. U. Ingold, *J. Am. Chem. Soc.*, 1981, **103**, 609.
129 D. Ma, J. Pan, L. Yin, P. Xu, Y. Gao, Y. Yin and Y. Zhao, *Org. Lett.*, 2018, **20**, 3455.
130 J. Gong and P. L. Fuchs, *J. Am. Chem. Soc.*, 1996, **118**, 4486.
131 J. Xiang, W. Jiang and P. L. Fuchs, *Tetrahedron Lett.*, 1997, **38**, 6635.
132 P. J. Stang and J. A. Bjork, *J. Chem. Soc. Chem. Commun.*, 1978, 1057.
133 T. Hoshikawa, S. Kamijo and M. Inoue, *Org. Biomol. Chem.*, 2012, **11**, 164.
134 Z.-F. Cheng, Y.-S. Feng, C. Rong, T. Xu, P.-F. Wang, J. Xu, J.-J. Dai and H.-J. Xu, *Green Chem.*, 2016, **18**, 4185.
135 J.-B. Han, H. H. San, A. Guo, L. Wang and X.-Y. Tang, *Adv. Synth. Catal.*, 2021, **363**, 2366.
136 M. Mella, M. Freccero, T. Soldi, E. Fasani and A. Albini, *J. Org. Chem.*, 1996, **61**, 1413.
137 M. Mella, M. Freccero and A. Albini, *Tetrahedron*, 1996, **52**, 5533.
138 A. Albini, M. Mella and M. Freccero, *Tetrahedron*, 1994, **50**, 575.
139 A. A. Fokin, P. R. Schreiner, N. A. Fokina, B. A. Tkachenko, H. Hausmann, M. Serafin, J. E. P. Dahl, S. Liu and R. M. K. Carlson, *J. Org. Chem.*, 2006, **71**, 8532.
140 A. A. Fokin, B. A. Tkachenko, P. A. Gunchenko, D. V. Gusev and P. R. Schreiner, *Chem. – Eur. J.*, 2005, **11**, 7091.
141 M. A. J. Duncton, *MedChemComm*, 2011, **2**, 1135.
142 I. Kavai, L. H. Mead, J. Drobniak and S. F. Zakrzewski, *J. Med. Chem.*, 1975, **18**, 272.
143 J. M. Anderson and J. K. Kochi, *J. Am. Chem. Soc.*, 1970, **92**, 1651.
144 A. Nayyar, V. Monga, A. Malde, E. Coutinho and R. Jain, *Bioorg. Med. Chem.*, 2007, **15**, 626.
145 D. H. R. Barton, B. Garcia, H. Togo and S. Z. Zard, *Tetrahedron Lett.*, 1986, **27**, 1327.
146 E. Castagnino, S. Corsano, D. H. R. Barton and S. Z. Zard, *Tetrahedron Lett.*, 1986, **27**, 6337.
147 A. P. Antonchick and L. Burgmann, *Angew. Chem. Int. Ed.*, 2013, **52**, 3267.
148 Q. Yang, P. Y. Choy, Y. Wu, B. Fan and F. Y. Kwong, *Org. Biomol. Chem.*, 2016, **14**, 2608.
149 D.-C. Wang, R. Xia, M.-S. Xie, G.-R. Qu and H.-M. Guo, *Org. Biomol. Chem.*, 2016, **14**, 4189.
150 X. Wang, B. Lei, L. Ma, L. Zhu, X. Zhang, H. Zuo, D. Zhuang and Z. Li, *Chem. – Asian J.*, 2017, **12**, 2799.
151 L. Zhou and H. Togo, *Eur. J. Org. Chem.*, 2019, **2019**, 1627.
152 H. Zhao, Z. Li and J. Jin, *New J. Chem.*, 2019, **43**, 12533.
153 I. B. Perry, T. F. Brewer, P. J. Sarver, D. M. Schultz, D. A. DiRocco and D. W. C. MacMillan, *Nature*, 2018, **560**, 70.
154 L. P. Ermolenko and C. Giannotti, *J. Chem. Soc. Perkin Trans. 2*, 1996, **0**, 1205.
155 O. Gutierrez, J. C. Tellis, D. N. Primer, G. A. Molander and M. C. Kozlowski, *J. Am. Chem. Soc.*, 2015, **137**, 4896.
156 A. K. Yadav and L. D. S. Yadav, *Org. Biomol. Chem.*, 2015, **13**, 2606.
157 Z.-Q. Zhu, T.-T. Wang, P. Bai and Z.-Z. Huang, *Org. Biomol. Chem.*, 2014, **12**, 5839.
158 Z. Li, Y. Zhang, L. Zhang and Z.-Q. Liu, *Org. Lett.*, 2014, **16**, 382.
159 D. Liang, B. Huo, Y. Dong, Y. Wang, Y. Dong, B. Wang and Y. Ma, *Chem. – Asian J.*, 2019, **14**, 1932.
160 J. Schörgenhumer and M. Waser, *Org. Chem. Front.*, 2016, **3**, 1535.
161 S. Kamijo, T. Hoshikawa and M. Inoue, *Org. Lett.*, 2011, **13**, 5928.
162 T. Hoshikawa, S. Yoshioka, S. Kamijo and M. Inoue, *Synthesis*, 2013, **45**, 874.
163 J.-P. Berndt, F. R. Erb, L. Ochmann, J. Beppler and P. R. Schreiner, *Synlett*, 2019, **30**, 493.
164 G. A. Olah, O. Farooq and G. K. S. Prakash, *Synthesis*, 1985, **1985**, 1140.
165 M.-X. Sun, Y.-F. Wang, B.-H. Xu, X.-Q. Ma and S.-J. Zhang, *Org. Biomol. Chem.*, 2018, **16**, 1971.
166 H. Peng, J.-T. Yu, Y. Jiang, H. Yang and J. Cheng, *J. Org. Chem.*, 2014, **79**, 9847.
167 W. K. Weigel, H. T. Dang, H.-B. Yang and D. B. C. Martin, *Chem. Commun.*, 2020, **56**, 9699.